

PISTON ACTUATED NASTIC MATERIALS

A Thesis

by

VIRAL SHAH

Submitted to the Office of Graduate Studies of
Texas A&M University
in partial fulfillment of the requirements for the degree of

MASTER OF SCIENCE

December 2008

Major Subject: Mechanical Engineering

PISTON ACTUATED NASTIC MATERIALS

A Thesis

by

VIRAL SHAH

Submitted to the Office of Graduate Studies of
Texas A&M University
in partial fulfillment of the requirements for the degree of

MASTER OF SCIENCE

Approved by:

Co-Chairs of Committee, Terry S. Creasy
J.N. Reddy

Committee Members, Zoubeida Ounaies
Head of Department, Dennis L. O'Neal

December 2008

Major Subject: Mechanical Engineering

ABSTRACT

Piston Actuated Nastic Materials. (December 2008)

Viral Shah, B.E., Andhra University, India

Co-Chairs of Advisory Committee: Dr. Terry S. Creasy
Dr. J.N. Reddy

This study investigated nastic materials applied to twisting a rigid beam. Nastic materials contain small, simple machines in a compliant matrix. Here a generic beam must twist by ± 4 degrees; the ± 4 degrees twist is an optimum value to change the angle of attack on a helicopter's rotor blade. Small piston actuators distributed through the beam's outer core provide the internal work needed. By actuating the piston elements in their axial direction, which is transverse to the beam's central axis, the beam twists as desired. This study's objective is to gain insight into the geometry, the material property combinations, and the boundary conditions that produce nastic materials and structures that twist. An important performance metric is the work density, which is the product of blocked stress and free strain. Blocked stress is the maximum actuation stress in a single stroke that produces maximum work output and free strain is the maximum actuation strain that produces the maximum work output.

Optimum work density was found for the piston actuators. As it is difficult to model distributed piston actuators across the beam's outer core, piston actuator's effective properties are calculated using finite element models and homogenized in the beam's outer core.

As the goal is to twist a beam, an important parameter in comparing the active beam

to a passive beam is torsional stiffness. Torsional stiffness is torque per unit deflection.

The active beam's torsional stiffness is 13.705 MN-m/rad without twist in the initial state, which is 3.5 times stiffer than the passive beam, and 13.341 MN-m/rad at the twisted state, which shows that the beam loses 2.6% of its stiffness during twist. The

passive beam's density is 1000.01 kg/m^3 and the active beam's density is 1399.42 kg/m^3 ,

which shows that active structures have a weight penalty that must be less than achieving the motion by traditional systems.

ACKNOWLEDGEMENTS

I would like to thank my research advisor Dr. Terry Creasy for his guidance, patience and support over the course of this research. This material is based upon work supported by Defense Advanced Research Projects Agency (DARPA) and the U.S. Army Research, Development and Engineering Command under contract W911 W6-04-C-0069.

I would also like to thank my committee members, Dr. J.N. Reddy and Dr. Zoubeida Ounaies for their efforts in reviewing and evaluating my research.

TABLE OF CONTENTS

	Page
ABSTRACT	iii
ACKNOWLEDGEMENTS	v
TABLE OF CONTENTS	vi
LIST OF FIGURES.....	viii
LIST OF TABLES	xii
1. INTRODUCTION.....	1
1.1. Overview	1
1.2. Objective	3
1.3. Scope of Thesis	4
2. BACKGROUND AND LITERATURE REVIEW.....	6
2.1. Actuator Requirements.....	9
2.1.1. Actuator Performance Characteristics.....	10
2.2. Hyperelastic Materials.....	12
2.2.1. Definitions and Basic Kinematic Results.....	13
2.2.2. Rate of Change of the Internal Virtual Work.....	17
2.2.3. Neo Hookean Material model	18
3. DESIGN AND EFFECTIVE PROPERTIES OF PISTON ACTUATOR.....	22
3.1. Piston Actuator Design.....	27
3.1.1. Blocked Stress for Different Material Properties	27
3.1.1.1. Boundary Conditions.....	28
3.1.1.2. Material Properties Used in Analysis.....	29
3.1.1.3. Element Selection.....	30
3.1.1.4. Numerical Results	30
3.1.2. Outer Diameter of Cylinder and Work Density	31
3.1.2.1. Boundary Conditions.....	33
3.1.2.2. Numerical Results	34
3.2. Effective Properties of Piston Actuator.....	37
3.2.1. Effect of Matrix Thickness on Effective Stiffness	40
3.2.1.1. Boundary Conditions.....	41
3.2.1.2. Element Selection.....	41

	Page
3.2.1.3. Material Properties and Constitutive Models Used in Analysis.....	43
3.2.1.4. Numerical Results	43
3.2.2. Effective in Plane Stiffness (E_2).....	44
3.2.3. Effective Transverse stiffness ($E_1=E_3$) and Poisson's ratio ($\nu_{13}, \nu_{21}=\nu_{23}$).....	46
3.2.3.1. Boundary Conditions.....	46
3.2.3.2. Numerical Results	47
3.2.4. Effective in Plane Shear Modulus (G_{23}).....	47
3.2.4.1. Boundary Conditions.....	48
3.2.4.2. Numerical Results	48
4. ANALYSIS OF GENERIC BEAM	51
4.1. Calculating Beam's Length to Negate End Boundary Conditions.....	52
4.2. Torsional Stiffness and Work Required to Twist Passive Beam	54
4.2.1. Boundary Conditions.....	54
4.2.2. Element Selection.....	55
4.2.3. Material Properties and Constitutive Model	55
4.2.4. Numerical Results	55
4.3. Torsional Stiffness of Active Beam	56
4.3.1. Material Properties and Constitutive Models Used.....	57
4.3.2. Element Selection.....	59
4.3.3. Numerical Results	59
4.4. Simulating Active Twist.....	60
4.4.1. Boundary Conditions.....	60
4.4.2. Element Selection.....	62
4.4.3. Material Properties and Constitutive Models Used.....	62
4.4.4. Numerical Results	62
4.4.5. Result Comparison	64
5. SUMMARY, CONCLUSIONS, AND FUTURE ACTIVITIES	65
REFERENCES	68
APPENDIX	71
VITA	74

LIST OF FIGURES

	Page
Figure 1. Conventional Control System, complex swash plate, bearings, linkages and push rods [5].	3
Figure 2. There are two control concept categories: Category I applies control forces are at the root, Category II applies control forces near the blade tip [1].	6
Figure 3. Higher harmonic motion (HHC) comes under Category I. HHC actively controls the rotor swashplate to change the blade pitch at the root [7].	7
Figure 4. Individual Blade Control uses control forces that are applied by using hydraulically activated pitch links to each blade individually [7].	7
Figure 5. In the trailing edge flap concept, the flap deflections induce lift and aerodynamic movements [7].	8
Figure 6. Actuation stress σ versus actuation strain ϵ for various actuators. This chart shows a medium for comparing actuators quantitatively.[8]	11
Figure 7. When experimental results—dots—and Neo-Hookean (2), Mooney Rivlin (3), and Hooke's (1) models appear together, it is evident that neo-hookean model is a good approximation. [11]	21
Figure 8. The concept behind twisting the generic beam is to generate two equal and opposite forces to twist the beam. One surface is fixed while the other end of the is subjected to two equal and opposite forces that makes the beam twist.	22
Figure 9. The generic beam is a 180x25 mm cross-section with an outer active core in between two Aluminum skins and inner core and spar. The actuators are placed in the outer active core.	23
Figure 10. The outer core has actuators distributed uniformly. The effective properties are found for the outer core using a representative volume element, which has a single actuator embedded in a matrix. Before finding the effective properties it is important to choose an actuator which has a high work density in the axial direction.	25

Figure 11. The senior piston/bellow acts as a basis to select the actuator for this application. This actuator is limited to the bellows' movement. This reduces the work density, which is blocked stress times free strain.	26
Figure 12. Axisymmetric piston model fixed at 1 x 2 mm represents a 2 mm diameter, 2 mm long rod.	28
Figure 13. To find the maximum blocked stress the bottom surface of the piston receives static pressure. The pressure increases until the piston yields. Four materials were analyzed and the pressure at blocked stress appears in the text.	29
Figure 14. The maximum pressure increases with increase in yield strength. This maximum pressure corresponds to the blocked stress for each material.	31
Figure 15. The cylinder bottom has a hemispherical shape that reduces stress concentration. The distances 1 and 2 remain equal. This simplifies the design process; however, the results shown here might not be optimal.	32
Figure 16. To find the optimum cylinder diameter, internal pressure is applied to the walls and work density is calculated at various diameters.	34
Figure 17. Work density reaches an optimum value as the outer diameter of the cylinder changes to support the operating pressure. At the highest possible operation pressure, the cylinder lacks volumetric efficiency.	35
Figure 18. Work density has an optimum value depending on the pressure, which varies from zero to the maximum allowable pressure before the piston starts yielding. In this case the optimum work density is 7.68 MJ/m^3	35
Figure 19. The work density for piston actuator depends on the diameter and the pressure. The 3-D chart here shows the optimum work density for aluminum material properties. The peak value is 7.68 MJ/m^3	36
Figure 20. The work density for the piston actuator increases with increasing yield strength. Maximum value is 42 MJ/m^3 for Steel and minimum value is 0.75 MJ/m^3 for Nylon material properties.	37
Figure 21. Representative volume element (RVE) used in analysis.	40

	Page
Figure 22. Boundary conditions used for the model of Section 3.2.1.1 are x-direction degrees of freedom are fixed on the outer matrix wall because there exists a symmetry plane and the y-direction degree of freedom on the bottom surface are set to zero. The upper surface has a fixed displacement in y-direction to calculate the stiffness.	42
Figure 23. The cylinder and piston head were perfectly bonded using the TIE command in ABAQUS, remaining surfaces have a frictionless surface-to-surface contact.	42
Figure 24. The effective stiffness is directly proportional to the matrix thickness.	44
Figure 25. Boundary conditions applied at Step 1 for the analysis of in plane effective stiffness (E_2) at 50% of piston stroke.	45
Figure 26. The piston is given a fixed y-displacement to move it to the required stroke, 100% in this case, and then a negative y displacement is given on the top matrix surface, the interactions between the piston and incompressible fluid and the incompressible fluid and cylinder are switched on.	46
Figure 27. A negative x displacement is given on the right surface and the bottom y surface is fixed in y displacement direction because symmetry exists and similarly bottom planes of 2 and 3 are fixed in y and z directions.	47
Figure 28. To calculate the shear modulus a complete model is taken as there are no symmetry planes. Boundary conditions to calculate the shear modulus are as shown in the figure.	48
Figure 29. Piston actuator's effective properties are used in the outer active core which is used to twist the beam.	50
Figure 30. The outer ends of the beam have maximum actuation. As we go towards the center the actuation decreases gradually and thus the result is a couple that helps in twisting the beam. The center part has no actuation and hence only stiffness at 0% is used.	52
Figure 31. The generic beam has one fixed end and the other end receives two equal and opposite forces that generate a couple.	53

Figure 32. To calculate the work required to twist the passive beam, the x and y displacements are set to zero on the inner surface and 1500 N load is applied at each node at the outer edge to twist the beam by 4 degrees. The ABAQUS TIE keyword bonds all the surfaces.	55
Figure 33. To calculate the torsional stiffness for an active beam at the initial position the active core is homogenized with the effective piston properties. The core is 50% piston actuators and 50% PU. Two equal and opposite forces act on the outer edges.	58
Figure 34. The contour map shows the vertical displacements in the beam.	59
Figure 35. To simulate the active twist in the beam, the beam is subjected to a temperature variation across the beam's length as shown.	61
Figure 36. To calculate the torsional stiffness at the final state of the beam, two equal and opposite forces are applied after the initial temperature test. The above contour shows vertical displacement after the initial temperature test.	61
Figure 37. This contour map shows displacements after the forces are applied to the beam.	64

LIST OF TABLES

	Page
Table 1. Typical actuator applications include aircraft, automobiles, and industrial machines [8].	10
Table 2. Common definitions used in this work to describe actuator performance.	12
Table 3. Material properties for four materials used to find blocked stress. Yield strength is the failure criterion. [13][14][15][16].	30
Table 4. Material properties used for the analysis of section 3.2.1 have appropriate modulus and Poisson's numbers.	43
Table 5. The Piston actuator's effective properties are transversely isotropic.	49
Table 6. These materials properties were used to analyze the generic beam.	54
Table 7. These material properties were used for the piston actuator in the outer core of the active beam.	58
Table 8. Effective material properties used for piston actuator that act as a transversely isotropic material.	63

1. INTRODUCTION

1.1. Overview

Recent technological challenges in the aerospace industry desire aircrafts that can change their structure's shape [1]. This technology helps reduce moving parts and hence performance compromises. To achieve this challenge aerospace needs a high-energy-density material that actively changes shape [1].

The dictionary defines nastic as “of or showing sufficiently greater cellular force or growth on one side of an axis to change the form or position of the axis.” [2]. Plants, like venus-fly-trap, that can rapidly adapt to changes in environment incorporate nastic movement. Nastic movements in plants can be reversible and repeatable movements in response to a stimulus, the movements are determined by the plant's anatomy. Nastic materials are emerging, high-energy-density materials based on plants nastic movement that acts as an answer to the aerospace need of a high-energy-density material [3].

Hawkins [4] introduced the concept through Machine Augmented Composites (MAC). In MAC, small-embedded machines replace fiber and particulate reinforcements. These machines can be any shape or size and modify force or motion in different ways. Nastic material thus allows for developing multifunctional properties, that is, multiple performance characteristics exist within a system.

This thesis follows the style of *International Journal for Numerical Methods in Fluids*.

These machines can act as actuators within a matrix and help in changing the material's shape. An actuator's design depends on the application's requirements and available methods for pressurizing the system internally. The actuator's shape provides maximum work energy density in the axial direction.

Nastic material's concept is applicable to helicopter rotor blades. Helicopters have complex and critical flight control devices. They have numerous bearings, linkages, push rods, and hinges. These components are costly and maintenance intensive. Many efforts to reduce the complexity have resulted in bearing-less and hinge-less rotors [5]. Figure 1 shows a conventional swashplate and push rod control system found on most helicopters. The cost, maintenance, and failure response for these components provide an impetus to search for alternative forms for main rotor pitch control.

The nastic concept might allow one to control helicopter blade twist by making the blades active. An actuator embedded in an outer core, which is an anisotropic material, makes the core active. Driving the actuator makes the blade twist so that the blade becomes a torsional actuator.

This work's purpose is to develop a computational piston actuated nastic material that behaves as a nastic core and aids in twisting a simple beam. This work investigates the geometry, the material property combinations, work required by an active core to twist a beam and actuator's distribution percentage. The torsional stiffness of an active beam in both the initial state and in the twisted state is compared to a passive beam.

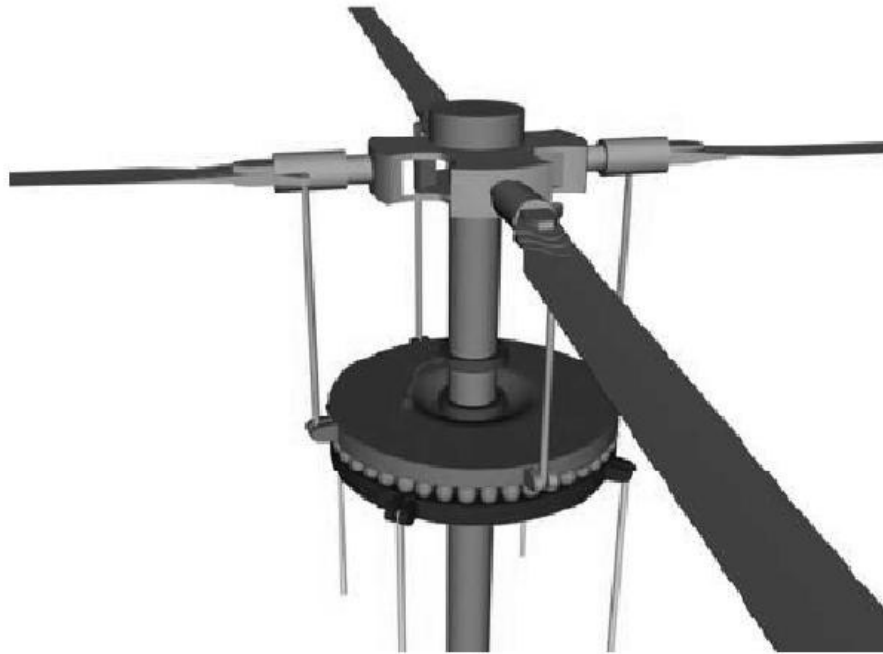


Figure 1. Conventional Control System, complex swash plate, bearings, linkages and push rods [5].

Section 2 covers the underlying principles for designing the actuator and the mathematical models used. Section 3 covers in detail the results, design, and actuator properties.

1.2. Objective

As we are trying to twist a stiff beam, this work's objective was to verify nastic materials capability in twisting stiff beams while maintaining the torsional stiffness. In addition, this analysis checks the weight penalty that nastic materials have in making the beam active.

Within this work a computational nastic core material model that would aid in twisting stiff beam structures such as helicopter rotor blades is developed. The work had

the following goals:

1. Study actuators with high deflection in the axial direction.
2. Use Senior Piston/Bellows system as baseline for actuator design.
3. Design actuator based on maximum strain, work energy density, and effect at sub-millimeter size.
4. Model actuator performance against static pressures.
5. Model embedded actuators in an elastomeric matrix and calculate the effective stiffness when the actuator is compressed against an incompressible fluid.
6. Find the performance penalty that embedding has on the material.
7. Study distributed actuator behavior in an active core by homogenizing the material.
8. Place this active core within a twist-actuated beam.
9. Compare the twist-actuated beam's performance to an equivalent passive beam's torsional stiffness.

1.3. Scope of Thesis

This thesis focuses on modeling a piston element based on the work required to twist a passive beam. Once modeled, the piston actuator's properties in an elastomeric matrix are found. Because it is difficult to model numerous piston elements and being computationally expensive the piston element properties are found numerically and are homogenized in the active beam to determine the torsional stiffness.

Subsequent sections present specific topics. Section 2 includes the background and literature review. Section 3 introduces the piston element design and analysis. Section 4

shows an active beam, and Section 5 presents conclusions from this work.

2. BACKGROUND AND LITERATURE REVIEW

Active control concepts fall into two main categories depending on the location where control forces occur. Figure 2 shows the categories.



Figure 2. There are two control concept categories: Category I applies control forces at the root, Category II applies control forces near the blade tip [1].

All blade actuation at the blade root classifies as Category I. Current research has two control concepts that come under category I, Higher harmonic control (HHC) and Individual Blade control (IBC) [1]. Higher harmonic control (HHC) uses active rotor swashplate control to change the pitch at the blade root. HHC uses the first rotor harmonic, which is the rotation frequency, and adds higher harmonic control motions. Figure 3 shows the HHC concept. [6] In IBC, hydraulically activated pitch links apply control forces to each blade individually. Figure 4 shows the IBC concept.

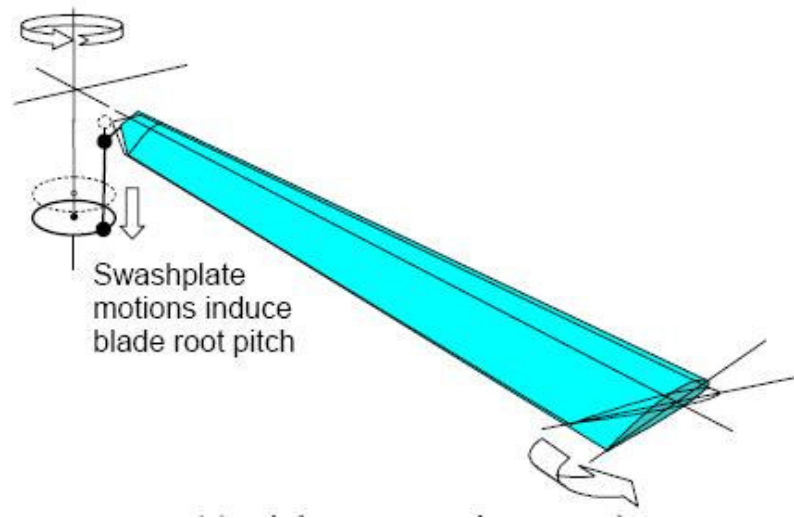


Figure 3. Higher harmonic motion (HHC) comes under Category I. HHC actively controls the rotor swashplate to change the blade pitch at the root [7].

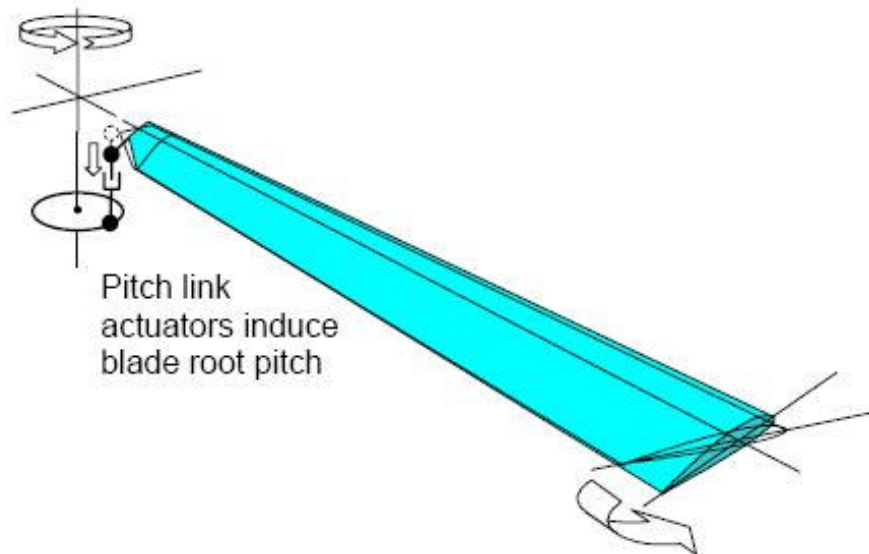


Figure 4. Individual Blade Control uses control forces that are applied by using hydraulically activated pitch links to each blade individually [7].

In the above concept control forces, traveling through the blade induces aerodynamic reaction. The aerodynamic forces are not steady state; the blade motion and aerodynamic forces are interdependent. This requires dynamic control inputs and hence this concept's real efficiency is not assessable.

Category II controls the aerodynamic forces that interact with blade motion.

Category II examples include the 'adaptive camber variation' that forces active cross-section deformation on rotor dynamics. [1] 'Trailing edge flap' is another concept where flap deflections induce lift and aerodynamic movements. Figure 5 shows the trailing edge flap's function.

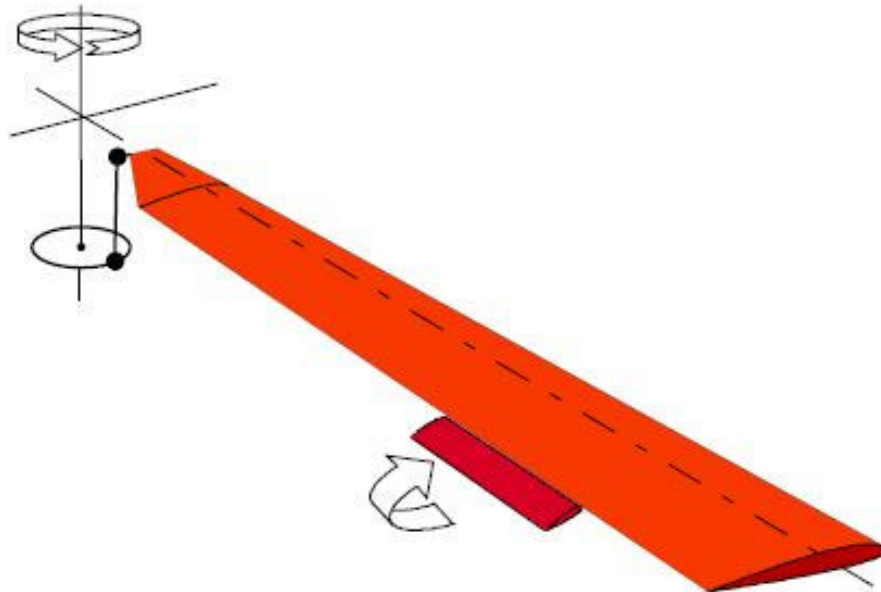


Figure 5. In the trailing edge flap concept, the flap deflections induce lift and aerodynamic movements [7].

However, efficiency in these concepts is questionable because flap movement changes lift distribution and causes additional vortices that might create losses.

Researchers developed another concept: active blade twist. [1] In this concept actuators in the blade's outer part actively twist the blade. On excitation, the actuators produce an axial force that deflects the rotor's outer part. Different actuator principles like servo-flaps and piezoelectric are used for active twist.

Finally, the actuator selected must provide necessary power, must work in static or dynamic use, must fit the installation space, and must have an appropriate specific mass. The present work has specific requirements that drive actuator selection.

2.1. Actuator Requirements

Actuators are the driving force for many fabricated and natural requirements. Table 1 shows the common uses. In each case, a control signal drives the mechanical action. Common actuator examples include animal muscles and plants, fabricated actuators include hydraulics and pneumatics. Recently, actuators made from shape changing materials are appearing in novel applications.

Table 1. Typical actuator applications include aircraft, automobiles, and industrial machines [8].

Aerospace	Flight control surfaces, landing gear movement, nose wheel steering, air brakes, powered doors/latches.
Automotive	Braking, active suspension, airbag deployment, etc.
Industrial Equipment	Numerically controlled machines, presses, lifting equipment, etc.

2.1.1. Actuator Performance Characteristics

Performance characteristics for an actuator must match the application requirements. Power, efficiency, force, displacement, etc define an application's requirement. The maximum actuation stress or blocked stress σ_{\max} , which is the maximum load that an active material can hold with no displacement and maximum actuation strain or free displacement ϵ_{\max} , which is the maximum displacement that can be generated at zero output load are the basic actuator characteristics. [8] The stress versus strain ($\sigma - \epsilon$) graph for an actuator is not a single curve but a family of curves that depend on the control signal and external constraints. Figure 6 shows ($\sigma - \epsilon$) curves for various actuators. The product $\sigma_{\max} \epsilon_{\max}$ estimates the work per unit volume in a single stroke. Table 2 lists definitions used in this analysis.

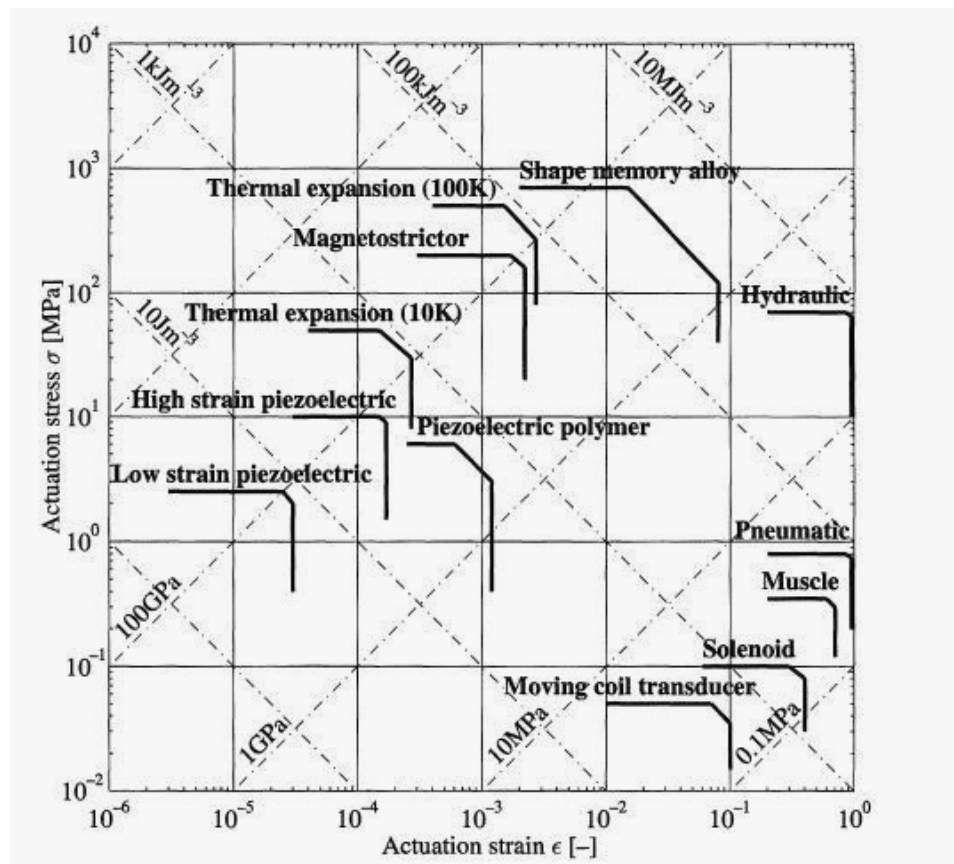


Figure 6. Actuation stress σ versus actuation strain ϵ for various actuators. This chart shows a medium for comparing actuators quantitatively [8].

Figure 6 provides a method for comparing actuators because the figure shows σ and ϵ combinations for each actuator. Actuators having significant free strain are on the figure's right side and these are suitable when high stroke is required in moving parts. The actuator near the top would be ideal for high force applications like the hydraulic rams. The top right hand corner actuators suit energy limiting tasks such as lifting weights.

Table 2. Common definitions used in this work to describe actuator performance.

Performance characteristic	Definition
Actuation stress σ	Applied force per unit area
Actuation strain (ϵ)	Nominal strain produced by an actuator
Maximum actuation stress(σ_{\max})	The maximum actuation stress in a single stroke that produces maximum work output
Maximum actuation strain(ϵ_{\max})	Maximum actuation strain that produces the maximum work output
Work Density (Work per unit volume)	The product maximum actuation stress times maximum actuation strain is the work density or work/unit volume.

2.2. Hyperelastic Materials

In hyperelastic materials, work is independent of the load path. [9] Existence of strain energy function that is a potential for the stress characterize a hyperelastic material.

$$S = \frac{2\partial\Psi(C)}{\partial C} \quad (1)$$

where ψ is the stored potential energy. [9] Many rubber-like materials have this

behavior. Understanding the formulations in this study require an introduction to the some basic definitions and kinematic results. This derivation follows from reference [10].

2.2.1. Definitions and Basic Kinematic Results

In this section the current material point position is called x and the reference position for the same material point is X . The deformation gradient F is

$$F = \frac{\partial x}{\partial X} \quad (2)$$

where F is the partial derivation in current position x with respect to the reference points X . The total volume change, J , at the point x is

$$J = \det \bar{F} \quad (3)$$

For simplicity, we define

$$F = J^{-\frac{1}{3}} \bar{F} \quad (4)$$

as this eliminates the deformation gradient with volume change. The deviatoric stretch matrix, the left Cauchy-green strain tensor, for F is

$$\bar{B} = \bar{F} \bar{F}^T \quad (5)$$

so that the first strain invariant is

$$\bar{I}_1 = \text{trace} \bar{B} = I : \bar{B} \quad (6)$$

where I_I is a unit matrix and the second strain invariant is

$$\bar{I}_2 = \frac{1}{2} (\bar{I}_1^2 - I : \bar{B} \bar{B}) \quad (7)$$

Some basic kinematic quantities must be discussed next. The gradient of displacement variation with respect to current position is

$$\partial L = \frac{\partial \delta v}{\partial x} \quad (8)$$

The symmetric part of ∂L is the virtual deformation rate:

$$\partial D = \text{sym}(\partial L) = \frac{1}{2}(\partial L + \partial L^T) \quad (9)$$

decomposing it into the virtual rate of change of volume per current volume—the virtual volumetric strain rate:

$$\delta \mathcal{E}^{vol} = I : \delta D \quad (10)$$

and virtual deviatoric strain rate,

$$\delta \mathcal{E} = \delta D - \frac{1}{3} \delta \mathcal{E}^{vol} I \quad (11)$$

∂L 's antisymmetric part is the virtual spin rate for the material and that is expressed by

$$\delta W = \text{asym}(\delta L) = \frac{1}{2}(\delta L - \delta L^T) \quad (12)$$

Variations of, $\overline{B}, \overline{B.B}, \overline{I}_1, \overline{I}_2$ and J are obtained from their definitions above

$$\delta \overline{B} = \delta e . \overline{B} + \overline{B} . \delta e + \delta W . \overline{B} - \overline{B} . \delta W = H_1 : \delta e + \delta W . \overline{B} - \overline{B} . \delta W \quad (13)$$

where

$$(H_1)_{ijkl} = \frac{1}{2}(\delta_{ik} \overline{B}_{jl} + \overline{B}_{ik} \delta_{jl} + \delta_{il} \overline{B}_{jk} + \overline{B}_{il} \delta_{jk}) \quad (14)$$

$$\begin{aligned} \delta(\overline{B.B}) &= \delta e . \overline{B.B} + \overline{B.B} . \delta e + 2 \overline{B} . \delta e . \overline{B} + \delta W . \overline{B.B} - \overline{B.B} . \delta W, \\ &= H_2 : \delta e + \delta W . \overline{B.B} - \overline{B.B} . \delta W \end{aligned} \quad (15)$$

where

$$(H_2)_{ijkl} = \frac{1}{2} (\delta_{ik} \bar{B}_{jp} \bar{B}_{pl} + \bar{B}_{ip} \bar{B}_{pk} \delta_{jl} + \delta_{il} \bar{B}_{jp} \bar{B}_{pk} + \bar{B}_{ip} \bar{B}_{pl} \delta_{jk}) + \bar{B}_{ik} \bar{B}_{jl} + \bar{B}_{il} \bar{B}_{jk} \quad (16)$$

$$\delta I_1 = 2 \bar{B} : \delta e; \quad (17)$$

$$\delta \bar{I}_2 = 2(\bar{I}_1 \bar{B} - \bar{B} \cdot \bar{B}) : \delta e \quad (18)$$

and

$$\delta J = J \delta \varepsilon^{vol} \quad (19)$$

Strain energy potential defines the Cauchy stress components as follows

Internal energy variation from virtual work principal is

$$\delta W_1 = \int_V \sigma : \delta D dV = \int_{V^o} J \sigma : \delta D dV^o \quad (20)$$

where V is the current volume, V_0 is the reference volume and σ are Cauchy stress components.

Equivalent pressure stress from the stress is

$$p = -\frac{1}{3} I : \sigma \quad (21)$$

and the deviatoric stress,

$$S = \sigma + pI \quad (22)$$

the internal energy variation thus becomes

$$\delta W_1 = \int_{V^o} J (S : \delta e - p \delta \varepsilon^{vol}) dV^o \quad (23)$$

For isotropic, compressible materials the strain energy, U , is a function of \bar{I}_1, \bar{I}_2 , and J

$$U = U(\bar{I}_1, \bar{I}_2, J) \quad (24)$$

and

$$\delta U = \frac{\partial U}{\partial I_1} \delta \bar{I}_1 + \frac{\partial U}{\partial I_2} \delta \bar{I}_2 + \frac{\partial U}{\partial J} \delta J \quad (25)$$

Hence using Equation(17), Equation (18) and Equation (19)

$$\delta U = 2[(\frac{\partial U}{\partial I_1} + \bar{I}_1 \frac{\partial U}{\partial I_2}) \bar{B} - \frac{\partial U}{\partial I_2} \bar{B} \cdot \bar{B}] : \delta e + J \frac{\partial U}{\partial J} \delta \mathcal{E}^{vol} \quad (26)$$

A variation of strain energy potential is internal virtual work per reference volume, δW_1

$$\delta W_1 = \int_{V^0} J(S : \delta e - p \delta \mathcal{E}^{vol}) dV^0 = \int_{V^0} \delta U dV^0, \quad (27)$$

For a compressible material, the strain variations are arbitrary, so this equation defines

the stress components for such a material as

$$S = \frac{2}{J} DEV[(\frac{\partial U}{\partial I_1} + \bar{I}_1 \frac{\partial U}{\partial I_2}) \bar{B} - \frac{\partial U}{\partial I_2} \bar{B} \cdot \bar{B}] \quad (28)$$

and

$$p = - \frac{\partial U}{\partial J} \quad (29)$$

For incompressible materials U is a function of \bar{I}_1 and \bar{I}_2 only and the internal energy in

augmented form is

$$(W_1)^A = \int_{V^0} [U - \hat{p}(J-1)] dV^0 \quad (30)$$

where \hat{p} is again a Lagrange multiplier. It is introduced to impose the constraint $J - 1 = 0$

so that variation of $(W_1)^A$ be taken to all kinematic variables. This gives

$$\delta(W_1)^A = \int [JS : \delta e - J \hat{p} \delta \mathcal{E}^{vol} - (J-1) \delta \hat{p}] dV^o \quad (31)$$

\hat{p} is interpolated in the same way as \hat{J} is interpolated, thus \hat{p} is assumed constant in first order elements to vary linearly with respect to position in second order elements.

2.2.2. Rate of Change of the Internal Virtual Work

Equation 1 defines deviatoric stress components S for pure displacement formulation of a compressible material. From S it can be shown that

$$d(JS) = J(C^S : de + Qd\mathcal{E}^{vol} + dW.S - S.dW) \quad (32)$$

where C^S defines the “effective deviatoric elasticity” of the material as

$$\begin{aligned} C^S = & \frac{2}{J} \left(\frac{\partial U}{\partial I_1} + \bar{I}_1 \frac{\partial U}{\partial \bar{I}_2} \right) H_1 - \frac{2}{J} \frac{\partial U}{\partial I_2} H_2 + \frac{4}{J} \left(\frac{\partial^2 U}{\partial \bar{I}_1^2} + 2\bar{I}_1 \frac{\partial^2 U}{\partial \bar{I}_1 \partial \bar{I}_2} + \bar{I}_1^2 \frac{\partial^2 U}{\partial \bar{I}_2^2} \right) \bar{B}\bar{B} \\ & - \frac{4}{J} \left(\frac{\partial^2 U}{\partial \bar{I}_1 \partial \bar{I}_2} + \bar{I}_1 \frac{\partial^2 U}{\partial \bar{I}_2^2} \right) (\bar{B}.\bar{B}\bar{B} + \bar{B}\bar{B}.\bar{B}) + \frac{4}{J} \frac{\partial^2 U}{\partial \bar{I}_2^2} \bar{B}.\bar{B}\bar{B}.\bar{B} \\ & - \frac{4}{3J} \left[\frac{\partial U}{\partial \bar{I}_1} + 2\bar{I}_1 \frac{\partial U}{\partial \bar{I}_2} + \bar{I}_1 \frac{\partial^2 U}{\partial \bar{I}_1^2} + (\bar{I}_1^2 + 2\bar{I}_2) \frac{\partial^2 U}{\partial \bar{I}_1 \partial \bar{I}_2} + 2\bar{I}_1 \bar{I}_2 \frac{\partial^2 U}{\partial \bar{I}_2^2} \right] (\bar{I}\bar{B} + \bar{B}\bar{I}) \\ & + \frac{4}{3J} \left(2 \frac{\partial U}{\partial \bar{I}_2} + \bar{I}_1 \frac{\partial^2 U}{\partial \bar{I}_1 \partial \bar{I}_2} + 2\bar{I}_2 \frac{\partial^2 U}{\partial \bar{I}_2^2} \right) (\bar{I}\bar{B}.\bar{B} + \bar{B}.\bar{B}\bar{I}) \end{aligned} \quad (33)$$

and Q defines deviatoric stress rate-volumetric strain rate coupling term,

$$Q = \frac{\partial(JS)}{\partial J} = 2 \left(\frac{\partial^2 U}{\partial \bar{I}_1 \partial J} + \bar{I}_1 \frac{\partial^2 U}{\partial \bar{I}_2 \partial J} \right) \bar{B} - 2 \frac{\partial^2 U}{\partial \bar{I}_2 \partial J} \bar{B}.\bar{B} - \frac{2}{3} \left(\bar{I}_1 \frac{\partial^2 U}{\partial \bar{I}_1 \partial J} + 2\bar{I}_2 \frac{\partial^2 U}{\partial \bar{I}_2 \partial J} \right) \bar{I}. \quad (34)$$

From Equation (28) it can be shown that

$$d(J_p) = -J(Q : de + Kd\mathcal{E}^{vol}) \quad (35)$$

where K is the effective bulk modulus of the material,

$$K = -\left(J \frac{\partial p}{\partial J} + p\right) = J \frac{\partial^2 U}{\partial J^2} + \frac{\partial U}{\partial J} \quad (36)$$

Thus,

$$\int \left[\delta e \cdot \delta \boldsymbol{\varepsilon}^{vol} \right] : \begin{pmatrix} C^s & Q \\ Q & K \end{pmatrix} : \left\langle \begin{matrix} de \\ d\boldsymbol{\varepsilon}^{vol} \end{matrix} \right\rangle - \boldsymbol{\sigma} : (2\delta \boldsymbol{\varepsilon} - \delta L^T \cdot dL) dV \quad (37)$$

because

$$\delta e : (dW \cdot S - S \cdot dW) + S : d\delta e - p d\delta \boldsymbol{\varepsilon}^{vol} = -\boldsymbol{\sigma} : (2\delta \boldsymbol{\varepsilon} - \delta L^T \cdot dL) \quad (38)$$

Rate of change of augmented variation of internal energy for incompressible materials is similarly obtained from Equation(31).

$$d\delta(W_I)^A = \int \left[\delta e \delta \boldsymbol{\varepsilon}^{vol} \delta \hat{p} \right] \begin{pmatrix} C^s & 0 & 0 \\ 0 & -\hat{p} & -1 \\ 0 & -1 & 0 \end{pmatrix} \left\{ \begin{matrix} de \\ d\boldsymbol{\varepsilon}^{vol} \\ d\hat{p} \end{matrix} \right\} - \boldsymbol{\sigma} : (2\delta \boldsymbol{\varepsilon} \cdot d\boldsymbol{\varepsilon} - \delta L^T \cdot dL) dV \quad (39)$$

2.2.3. Neo Hookean Material model

Many strain energy potential forms are available like the Mooney-Rivlin form, Neo-Hookean form, Odgen form, Vander Waals form, Yeoh form etc.

This study uses only the Neo-Hookean form because it is the simplest and requires minimal experimental data.

For incompressible or almost incompressible behavior, we can write the potential as

$$U = f(\bar{I}_1 - 3, \bar{I}_2 - 3) + g(J_{el} - 1) \quad (40)$$

Setting $g = \sum \frac{1}{D_i} (J_{el} - 1)^{2i}$ and expanding $f(\bar{I}_1 - 3, \bar{I}_2 - 3)$ in a Taylor series, we

arrive at

$$U = \sum_{i+j=1}^N C_{ij} (\bar{I}_1 - 3)^i (\bar{I}_2 - 3)^j + \sum_{i=1}^N \frac{1}{D_i} (J_{el} - 1)^{2i} \quad (41)$$

This is a polynomial representation for strain energy potential. The parameter N takes values up to six. If both first and second invariants are taken into account, values greater than 2 are usually not used. C_{ij} and D_i are temperature-dependent material parameters. The user specifies values for N , C_{ij} and D_i as functions of temperature. The elastic volume strain, J_{el} , follows from the total volume strain, J , and the thermal volume strain, J_{th} , with the relation

$$J_{el} = \frac{J}{J_{th}} \quad (42)$$

and J_{th} follows from the linear thermal expansion, ε_{th} with

$$J_{th} = (1 + \varepsilon_{th})^3 \quad (43)$$

where ε_{th} follows from the temperature and the isotropic thermal expansion coefficient defined by the user.

The D_i values determine the material's compressibility. For fully incompressible materials D_i is zero for all i . If $D_1=0$, all D_i must be zero.

Regardless of N , the initial shear modulus, μ_0 and the bulk modulus, κ_0 depend only on the polynomial coefficients of order $N=1$

$$\mu_0 = 2(C_{10} + C_{01}) , \kappa_0 = \frac{2}{D_1} \quad (44)$$

If $N=1$, the Mooney-Rivlin form is recovered

$$U = C_{10}(\bar{I}_1 - 3) + C_{01}(\bar{I}_2 - 3) + \frac{1}{D_1}(J_{el} - 1)^2 \quad (45)$$

The Mooney-Rivlin form is an extension to the Neo-Hookean form as it adds a term that depends on second invariant of the left Cauchy-Green tensor.

If all C_{ij} with $j \neq 0$ are set to zero, the reduced polynomial form is

$$U = \sum_{i=1}^N C_{i0}(\bar{I}_1 - 3)^i + \sum_{i=1}^N \frac{1}{D_i}(J_{el} - 1)^{2i} \quad (46)$$

If the reduced-polynomial strain-energy function is simplified by setting $N=1$, the Neo-Hookean form is obtained

$$U = C_{10}(\bar{I}_1 - 3) + \frac{1}{D_1}(J_{el} - 1)^2 \quad (47)$$

Both Neo-Hookean and Mooney-Rivlin form usually give similar accuracy because they use only linear invariant functions. Figure 7 shows a comparison between the two and experimental data.

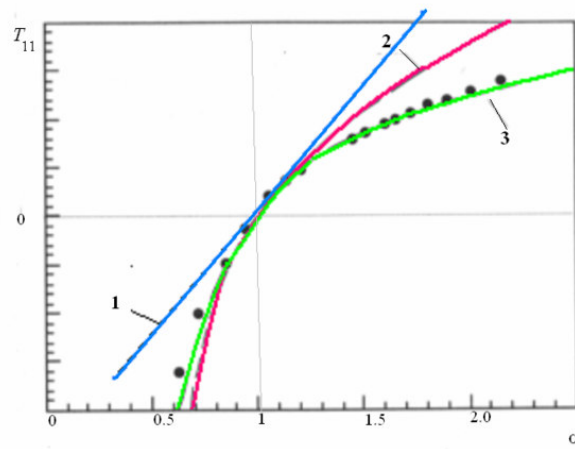


Figure 7. When experimental results—dots—and Neo-Hookean (2), Mooney Rivlin (3), and Hooke's (1) models appear together, it is evident that neo-hookean model is a good approximation [11].

3. DESIGN AND EFFECTIVE PROPERTIES OF PISTON ACTUATOR

Although the contract objective is to twist a helicopter's rotor blade, a generic beam can show the potential and limits for twisting a structure. This generic beam is a simplified, rectangular, thin-walled structure.

In order to twist the beam, embedded actuators in an outer active core are distributed uniformly. These actuators are placed such that when actuated in their axial direction through internally generated pressure, it creates equal and opposite forces on the beam that twists the beam. Figure 8 shows the basic concept.

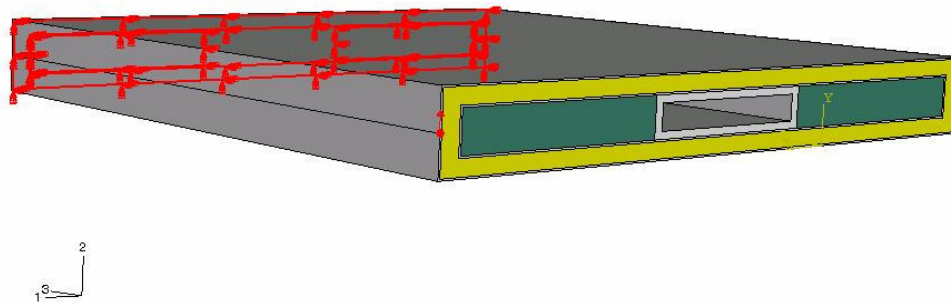


Figure 8. The concept behind twisting the generic beam is to generate two equal and opposite forces to twist the beam. One surface is fixed while the other end of the is subjected to two equal and opposite forces that makes the beam twist.

The generic beam is 180 mm x 25 mm and consists of an active core—the outer core, an inner core, a spar and aluminum skins. Aluminum skins bound the outer core. The

inner core uses Rohacell [20] material properties. Rohacell is a closed cell rigid foam plastic based on polymethacrylimide (PMI), it is widely used in the automotive and aerospace industry. Spar uses aluminum properties. Both the spar and inner core increase the beam's stiffness. The beam has tensile strength in Z direction, bending stiffness about X and torsional stiffness about Z. Figure 9 shows the beam's cross-section and how the actuators are distributed across the active core.

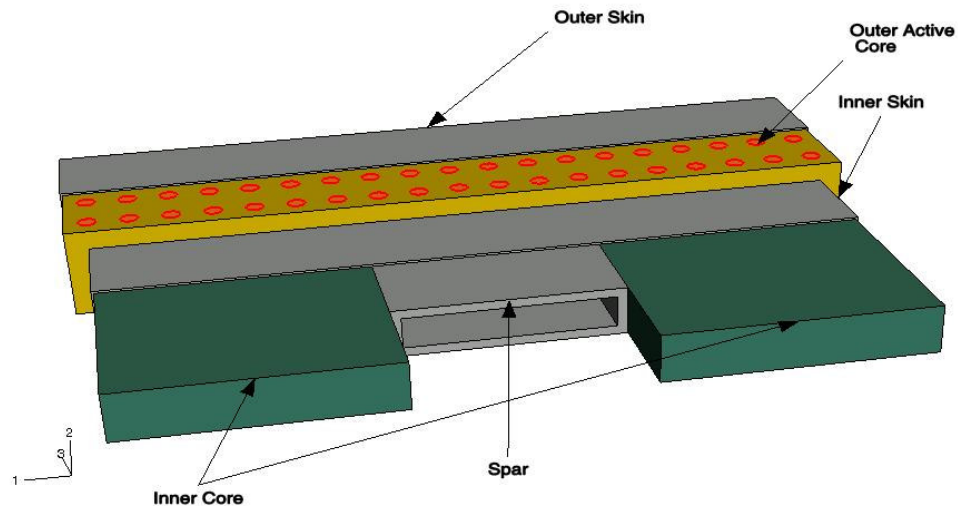


Figure 9. The generic beam is a 180x25 mm cross-section with an outer active core in between two Aluminum skins and inner core and spar. The actuators are placed in the outer active core.

In order to create an active beam with high torsional stiffness it is important to design actuators that have high work density in the axial direction. The work required to twist a passive beam by ± 4 degrees is calculated and this helps in choosing the right

work density for an actuator.

As modeling numerous actuators in the outer core is both difficult and computationally expensive, a single actuator's effective properties are calculated using a representative volume element (RVE). RVE consists of a single actuator embedded in a compliant matrix. Before finding the effective properties, it is important to design the right actuator for the application. Figure 10 shows how the RVE is devised from the outer active core's model. Further sections explain in detail the design, effective properties of a single actuator.

As explained an actuator is the driving force in twisting the beam. Thus modeling an actuator is the first important step. Because the axial force generates the twisting moment, an actuator having maximum work density in the axial direction is required. To achieve this, a senior piston/bellows model [12] served as a basis to model the actuator.

Figure 11 shows senior piston/bellow's model actuator. In this model, internal pressure moves the piston in the axial direction. The piston's movement is then limited to the number of convolutions on the bellow. This restricts the actuator's strain to the bellow's movement.

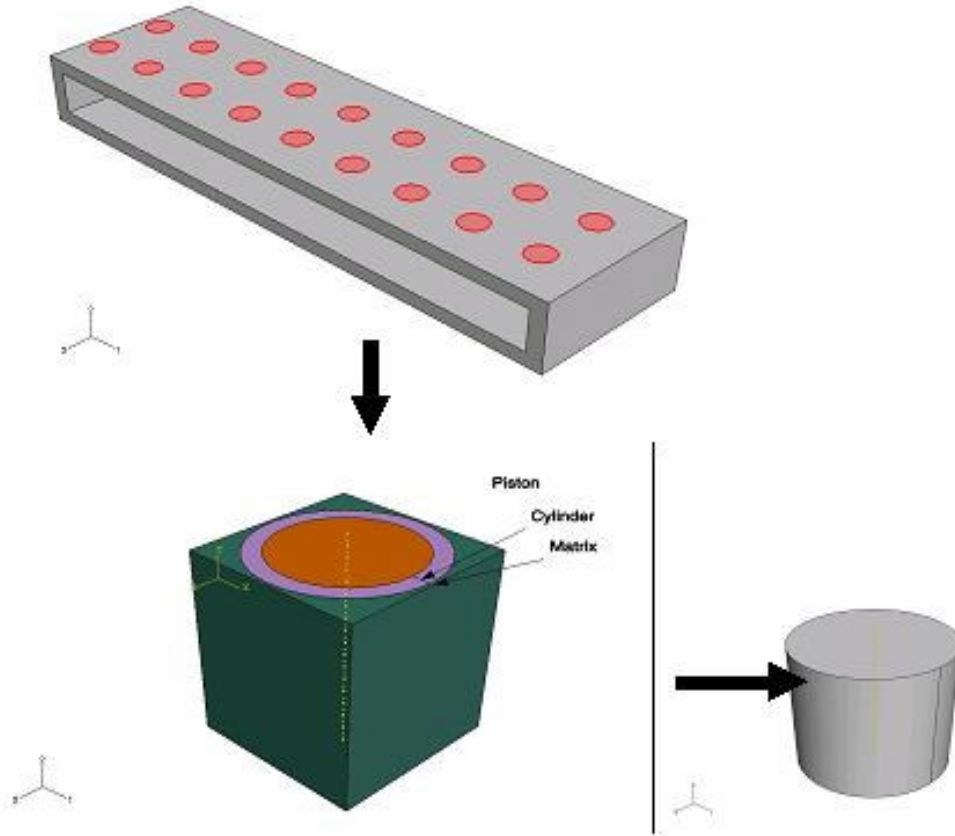


Figure 10. The outer core has actuators distributed uniformly. The effective properties are found for the outer core using a representative volume element, which has a single actuator embedded in a matrix. Before finding the effective properties it is important to choose an actuator which has a high work density in the axial direction.

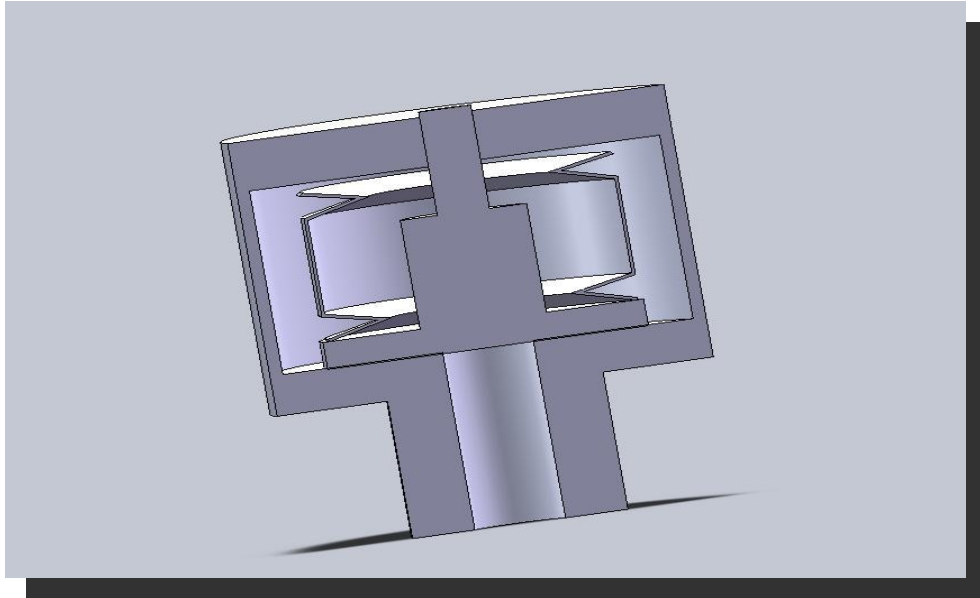


Figure 11. The senior piston/bellow acts as a basis to select the actuator for this application. This actuator is limited to the bellows' movement. This reduces the work density, which is blocked stress times free strain.

Section 0 defines an actuator's performance characteristics as blocked stress, σ_{\max} and free strain, ϵ_{\max} . While the model shown above would have high blocked stress, the free strain is limited to the bellow's movement, which in this case is less. The system's overall work density reduces. A piston actuator in comparison to a piston/bellow actuator has a high potential for better work density due to the high strain. A piston can have up to 100% strain, which corresponds to the piston's stroke.

Various methods are available to generate internal pressure for the actuator including phase change, electro-osmosis, and gas generation. In this analysis, an incompressible fluid acts as the driving force to actuate the piston element. The incompressible fluid simplifies the analysis and saves computational time.

The design and piston's effective properties appear in two sections. First with finite

element models, the optimum work density for four materials is calculated. These materials vary in their yield strength. The amount of work required to twist a passive beam acts as a basis for choosing the work density for an actuator. Thus the materials yield strength values varies from low values as in Nylon to high values as in Steel. This then gives a database of available work densities from which an appropriate actuator can be chosen for an application. Secondly, piston's effective properties once embedded in an elastomeric matrix come from finite element models.

3.1. Piston Actuator Design

To model the piston actuator the blocked stress and free strain are calculated. The product $\sigma_{\max} \varepsilon_{\max}$ gives the work density. The piston actuator is then designed for optimum work density.

3.1.1. Blocked Stress for Different Material Properties

Because there are many parameters associated with modeling a piston actuator, as a starting point, the piston's size is fixed and the cylinder's outer diameter is found for optimum work density. To choose a right size for the piston both miniaturization and the ability to produce these was kept in mind. The piston's fixed size is 2 mm height and 2 mm diameter. Figure 12 shows a 2-D axisymmetric piston model used in the analysis.

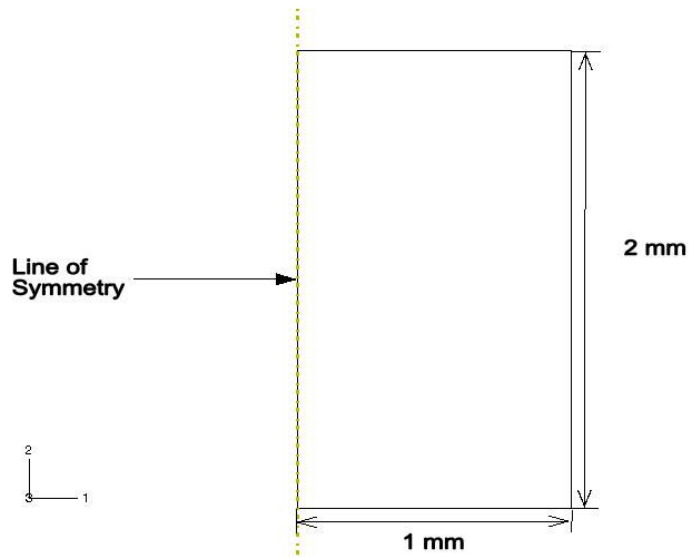


Figure 12. Axisymmetric piston model fixed at 1 x 2 mm represents a 2 mm diameter, 2 mm long rod.

This finite element model above provides the blocked stress. The failure criterion chosen was the material's yield stress. The material model is perfectly elastic-plastic, which has no hardening zone. The pressure that fails the material is the maximum pressure for cylinder design. ABAQUS 6.6, finite element analysis software was used for analysis.

3.1.1.1. Boundary Conditions

Figure 13 shows the boundary conditions used. On the bottom surface, a uniform pressure acts and the pressure increases until the piston yields. This maximum working pressure sets the outer cylinder diameter. Because the whole system is cylindrical with a line of symmetry at the center, an axisymmetric model is used.

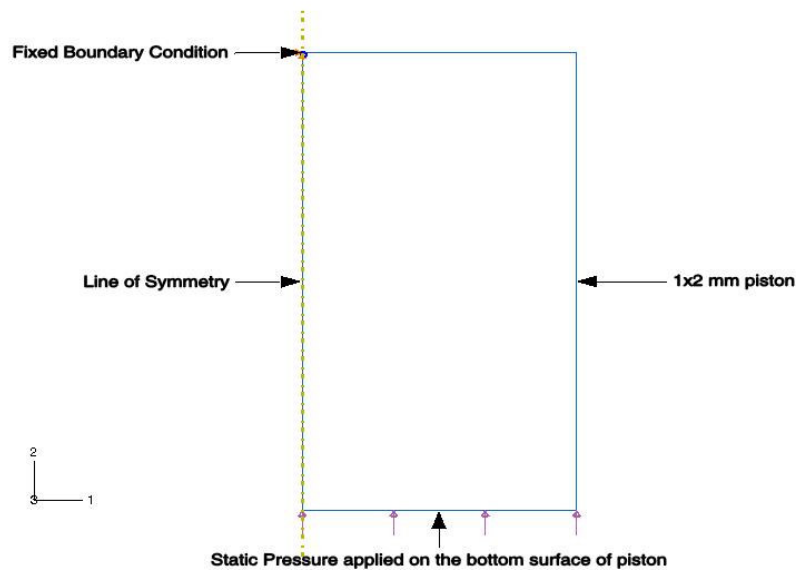


Figure 13. To find the maximum blocked stress the bottom surface of the piston receives static pressure. The pressure increases until the piston yields. Four materials were analyzed and the pressure at blocked stress appears in the text.

3.1.1.2. Material Properties Used in Analysis

Table 3 shows properties for four materials. Maximum pressure for each material is calculated. The material is isotropic. The length unit used for the model was millimeter. Thus, all moduli were input in MPa. This produces momentum equations with N/mm^3 units.

Table 3. Material properties for four materials used to find blocked stress. Yield strength is the failure criterion. [13][14][15][16]

Material	Modulus of Elasticity (MPa)	Yield Strength (MPa)	Poisson's Ratio
Nylon	2000	66	0.35
PEEK	3500	80	0.40
Aluminum	73000	103	0.33
Steel	200000	305	0.29

3.1.1.3. Element Selection

CAX4R a four-node bilinear axisymmetric quadrilateral element was used to model the piston actuator.

3.1.1.4. Numerical Results

Figure 14 shows maximum pressure against material's yield strength. The maximum pressure obtained is almost equal to material's yield strength.

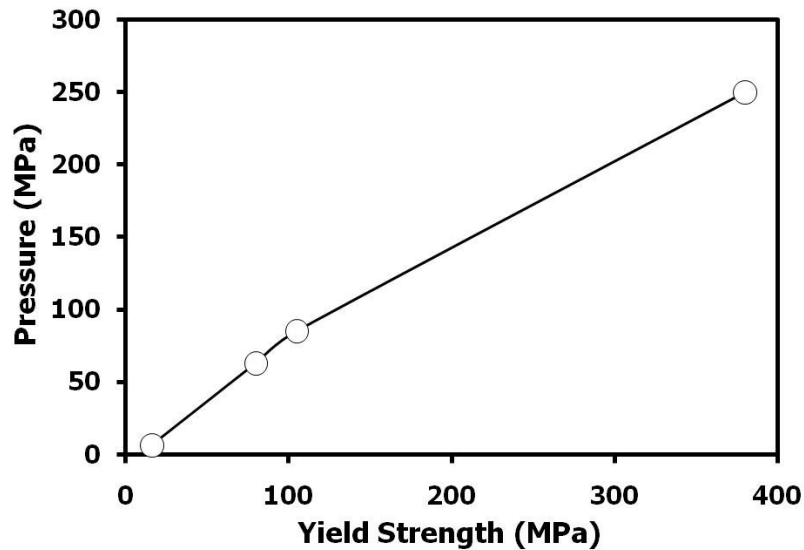


Figure 14. The maximum pressure increases with increase in yield strength. This maximum pressure corresponds to the blocked stress for each material.

3.1.2. Outer Diameter of Cylinder and Work Density

The maximum pressure found in previous section sets a target pressure that the cylinder's outer diameter must contain for optimum work density. There exists an optimum work density because, if the maximum pressure drives the cylinder design, the cylinder walls will be thick. As work density is work per unit volume the work density decreases appreciably due to the huge volume. Similarly, if a thin wall is used, the volume will decrease but it would hold less pressure and again the work density decreases appreciably. Therefore somewhere between these extremes lies an optimum diameter or thickness for the piston actuator.

To achieve this, the maximum pressure was applied to cylinder's inner walls and the thickness is calculated. Now the pressure value decreases all the way to zero at regular intervals. The thickness and work density at each interval is calculated. The local

maximum in the work density curve is the optimum work density for the particular material.

Figure 15 shows cylinder's model and dimensions used in the analysis. The semi-circular arc near the cylinder's bottom decreases stress concentration. In addition, the wall's thickness at the points marked in the Figure as 1 and 2 remain equal.

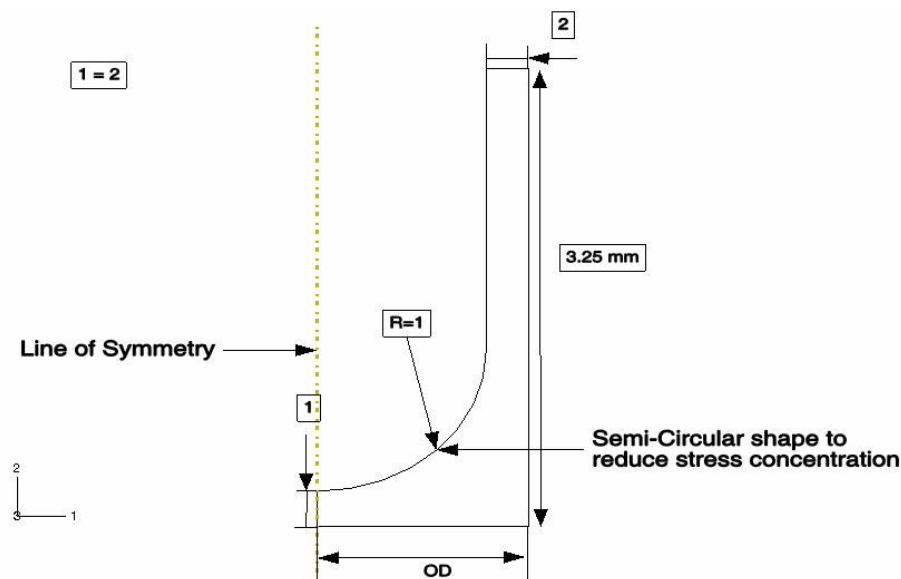


Figure 15. The cylinder bottom has a hemispherical shape that reduces stress concentration. The distances 1 and 2 remain equal. This simplifies the design process; however, the results shown here might not be optimal.

Work density is the product $\sigma_{\max} \varepsilon_{\max}$. Change in length, Δl , in this case is taken as 90% of piston stroke, which is $2 \times 0.9 = 1.8\text{mm}$. A model work-density calculation appears below,

$$P = 15\text{MPa}$$

$$\varepsilon = 1.8\text{mm}/2\text{mm}=0.9$$

$$A = \pi * 1 = \pi \text{ mm}^2$$

$$D = 2.5 \text{ mm}$$

$$V = 11.045 \text{ mm}^3$$

Work Density = Work/Volume

$$\text{Work} = \sigma_{\max} \varepsilon_{\max}$$

$$= F/A * \varepsilon_{\max}$$

$$\text{Work Density} = ((P * A * \Delta l) / V)$$

$$= (15 * \pi * 1.8) / 11.045$$

$$= 7.68 \text{ MJ/mm}^3$$

Where P is the pressure applied, A is the surface area, and D is the cylinder's outer diameter.

3.1.2.1. Boundary Conditions

Figure 16 shows the boundary conditions. Uniform pressure acts on the cylinder's inner walls. One node on the bottom surface has x and y displacement directions set to zero.

The first analysis uses aluminum properties. The material is isotropic. A 2-D axisymmetric model having CAX4R element is used for analysis. Work density is calculated for three other materials whose properties are in Table 3.

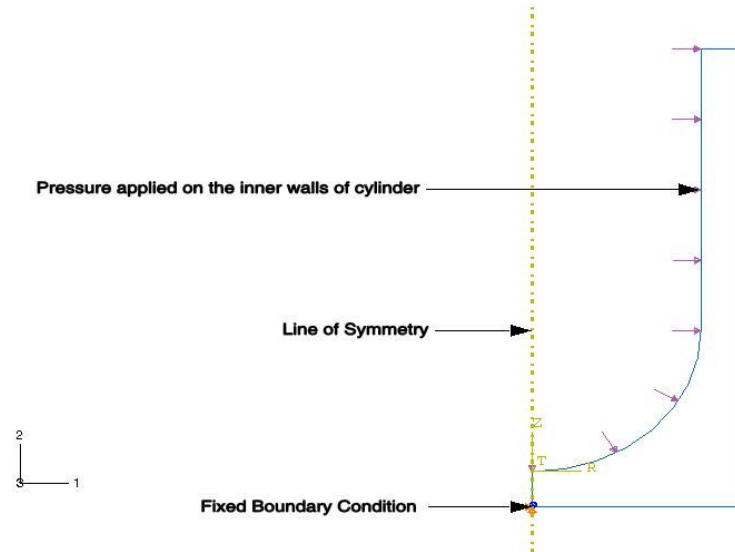


Figure 16. To find the optimum cylinder diameter, internal pressure is applied to the walls and work density is calculated at various diameters.

3.1.2.2. Numerical Results

Figure 17 shows the work density compared to diameter and Figure 18 shows the work density compared to pressure. The optimum work density for aluminum is 7.68MJ/m^3 .

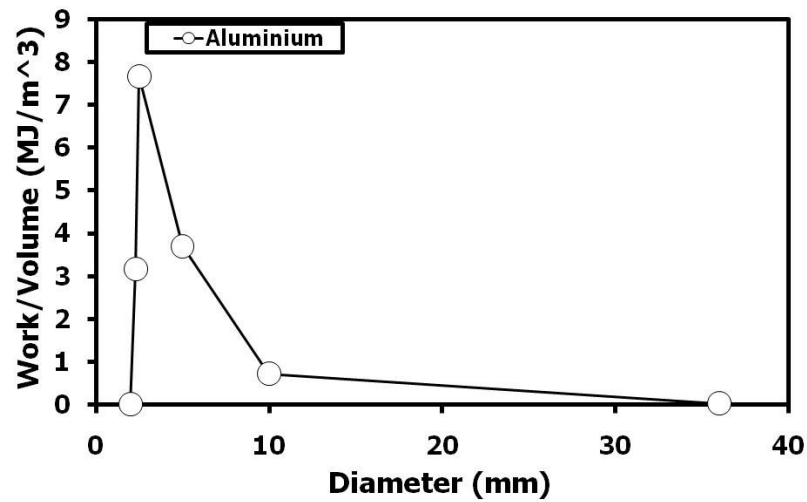


Figure 17. Work density reaches an optimum value as the outer diameter of the cylinder changes to support the operating pressure. At the highest possible operation pressure, the cylinder lacks volumetric efficiency.

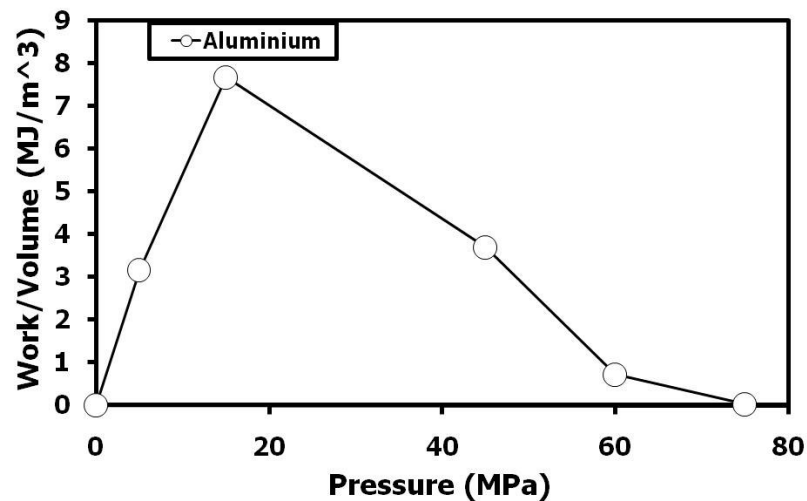


Figure 18. Work density has an optimum value depending on the pressure, which varies from zero to the maximum allowable pressure before the piston starts yielding. In this case the optimum work density is 7.68 MJ/m³.

Figure 19 shows a 3-D chart; in this chart optimum work density depends on pressure and cylinder outer diameter. The optimum outer diameter is 2.5mm and the maximum value is 100mm for aluminum material properties. The optimum pressure is 15 MPa. Figure 20 shows that work density increases as material yield strength increases. Because the free strain is constant for this piston, the work density depends on the blocked stress, which is the piston's failure stress limits.

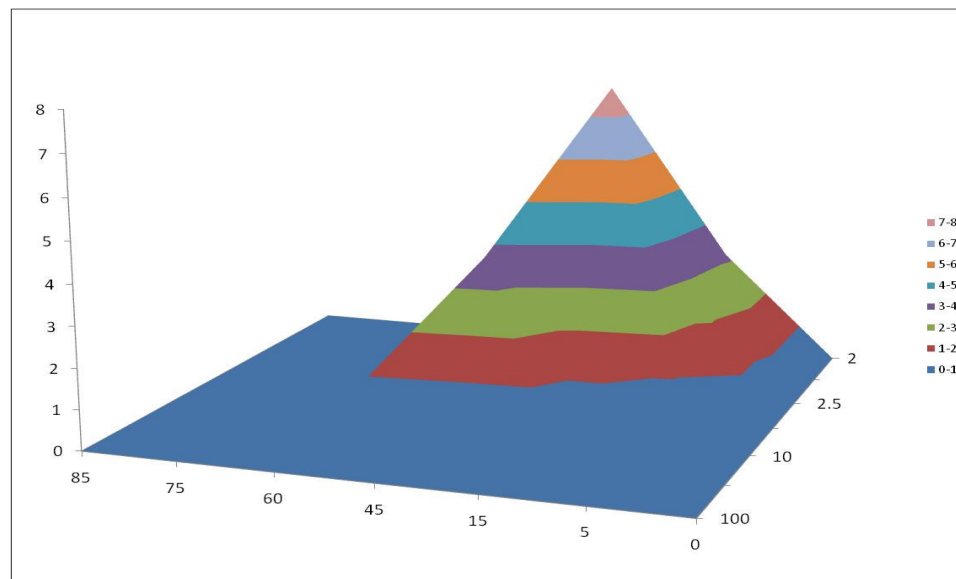


Figure 19. The work density for piston actuator depends on the diameter and the pressure. The 3-D chart here shows the optimum work density for aluminum material properties. The peak value is 7.68 MJ/m³.

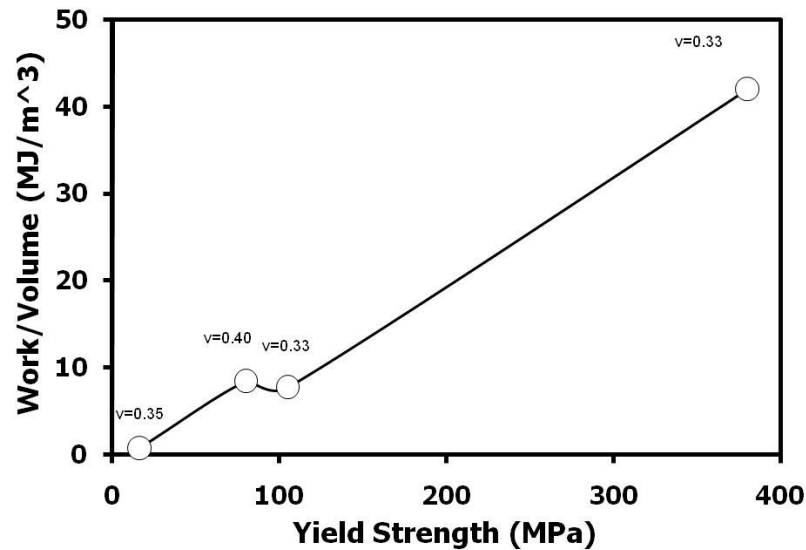


Figure 20. The work density for the piston actuator increases with increasing yield strength. Maximum value is 42 MJ/m³ for Steel and minimum value is 0.75 MJ/m³ for Nylon material properties.

The work density for various materials gives a database and an estimate as to how the work density for piston actuator's change with respect to yield strength. Once the work required to twist a beam is calculated, the work density for the piston actuators is easy to select from the database. The work density depends on the application. The maximum work density obtained is 42MJ/m³ for Steel.. The piston's density also plays an important factor due to the weight penalty. The minimum work density obtained is 0.75 MJ/m³ for Nylon. Appendix has the results for other materials.

3.2. Effective Properties of Piston Actuator

In orthotropic materials, linear elasticity is best described by giving the engineering constants: the three moduli E_1 , E_2 , E_3 ; Poisson's ratio ν_{12} , ν_{13} , ν_{23} ; and the shear moduli G_{12} , G_{13} and G_{23} [17], each associated to the material's principal direction. These

moduli define elastic compliance according to

$$\begin{bmatrix} \varepsilon_{11} \\ \varepsilon_{22} \\ \varepsilon_{33} \\ \varepsilon_{12} \\ \varepsilon_{13} \\ \varepsilon_{23} \end{bmatrix} = \begin{pmatrix} \frac{1}{E_1} & \frac{-\nu_{21}}{E_2} & \frac{\nu_{31}}{E_3} & 0 & 0 & 0 \\ \frac{-\nu_{12}}{E_1} & \frac{1}{E_2} & \frac{-\nu_{32}}{E_3} & 0 & 0 & 0 \\ \frac{-\nu_{13}}{E_1} & \frac{\nu_{23}}{E_2} & \frac{1}{E_3} & 0 & 0 & 0 \\ 0 & 0 & 0 & \frac{1}{G_{12}} & 0 & 0 \\ 0 & 0 & 0 & 0 & \frac{1}{G_{13}} & 0 \\ 0 & 0 & 0 & 0 & 0 & \frac{1}{G_{23}} \end{pmatrix} \begin{bmatrix} \sigma_{11} \\ \sigma_{22} \\ \sigma_{33} \\ \sigma_{12} \\ \sigma_{13} \\ \sigma_{23} \end{bmatrix} \quad (48)$$

ν_{ij} is the Poisson's ratio that characterizes the transverse strain in j direction when the material is stressed in i direction. In general ν_{ij} and ν_{ji} are related as

$$\frac{\nu_{ij}}{E_i} = \frac{\nu_{ji}}{E_j} \quad (49)$$

One special orthotropic case is a transversely isotropic material--isotropy exists at every material point in the transverse plane. The stress-strain laws reduce to

$$\begin{bmatrix} \epsilon_{11} \\ \epsilon_{22} \\ \epsilon_{33} \\ \epsilon_{12} \\ \epsilon_{13} \\ \epsilon_{23} \end{bmatrix} = \begin{pmatrix} \frac{1}{E_p} & \frac{-\nu_p}{E_p} & \frac{\nu_{tp}}{E_t} & 0 & 0 & 0 \\ \frac{-\nu_p}{E_p} & \frac{1}{E_p} & \frac{-\nu_{tp}}{E_t} & 0 & 0 & 0 \\ \frac{-\nu_{13}}{E_1} & \frac{\nu_{23}}{E_2} & \frac{1}{E_3} & 0 & 0 & 0 \\ 0 & 0 & 0 & \frac{1}{G_p} & 0 & 0 \\ 0 & 0 & 0 & 0 & \frac{1}{G_t} & 0 \\ 0 & 0 & 0 & 0 & 0 & \frac{1}{G_t} \end{pmatrix} \begin{bmatrix} \sigma_{11} \\ \sigma_{22} \\ \sigma_{33} \\ \sigma_{12} \\ \sigma_{13} \\ \sigma_{23} \end{bmatrix} \quad (50)$$

Assuming 1-2 plane to be the isotropy plane, transverse isotropy requires that $E_1=E_2=E_p$ and $\nu_{31} = \nu_{32} = \nu_{tp}$, $\nu_{13}=\nu_{23} =\nu_{pt}$ and $G_{13}=G_{23}=G_t$, where p and t stand for in-plane and transverse, respectively. G_p is given by

$$G_p = \frac{E_p}{2(1+\nu_p)} \quad (51)$$

The stability of transversely isotropic materials is given by

$$E_p, E_t, G_p, G_t > 0$$

$$\nu_p < 1$$

$$\nu_{pt} < (E_p/E_t)$$

$$\nu_{tp} < (E_t/E_p)$$

$$1 - \nu_p^2 - 2\nu_{tp}\nu_{pt} - 2\nu_p\nu_{tp}\nu_{pt} > 0$$

The piston actuator model is a transversely isotropic material and thus the effective five engineering constants are required. The effective properties come from modeling the piston as a representative volume element and subjecting that element to the required

boundary conditions. The matrix above and below the piston and cylinder also plays a major part, thus matrix thickness effect is analyzed. The piston actuator is 70% of the total volume.

Figure 21 shows a representative volume element (RVE) used for one analysis. The RVE consists of a piston, a cylinder, an incompressible fluid, and a matrix.

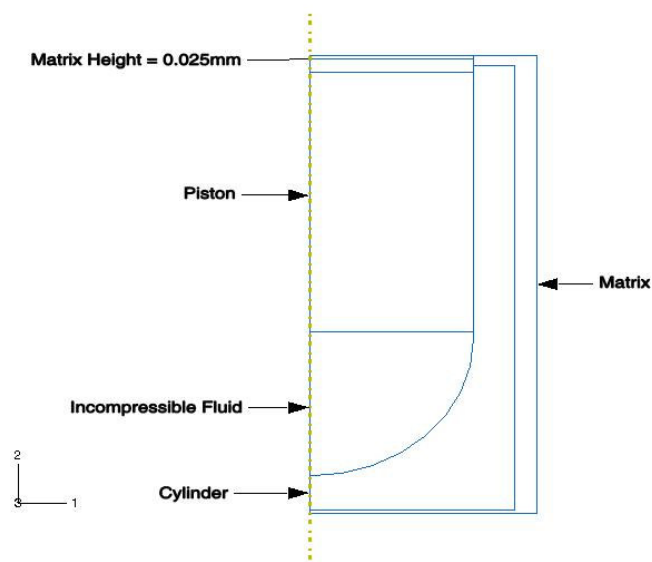


Figure 21. Representative volume element (RVE) used in analysis.

3.2.1. Effect of Matrix Thickness on Effective Stiffness

The matrix thickness above the piston head changes effective stiffness. The effective stiffness comes from compressing the piston against the incompressible fluid. The stress values are the top surface nodal y-reaction forces divided by the top surface area. The strain values are the top surface y-displacement values divided by the original model height.

3.2.1.1. Boundary Conditions

Figure 22 shows the boundary conditions applied. -0.0355 mm y-displacement moves the top surface and the initial matrix thickness is 0.025 mm. The thickness height increases from 0.050mm to 0.075mm to find the matrix thickness effect on stiffness. Because the whole system is cylindrical, a symmetry line exists at the center; therefore, an axisymmetric model is used.

The bottom surface has y-displacement degree-of-freedom set to zero. The small vertical edge on the incompressible fluid has x displacements set to zero to avoid penetration into the cylinder. Because this system is in a large piston/matrix element array, the outer vertical edge is a symmetry plane and thus the x-displacements of this edge are zero.

3.2.1.2. Element Selection

CAX4R, a 2D 4-node axisymmetric quadrilateral element is used for the piston and cylinder. CAX4H a 2D four node axisymmetric quadrilateral element with hybrid formulation is used for the matrix and incompressible fluid. The hybrid formulation is used for incompressible fluids [17]. The matrix and piston surfaces are perfectly bonded using the TIE command in ABAQUS 6.6. All the other parts have a surface-to-surface frictionless contact. Figure 23 shows the different contacts used in the analysis.

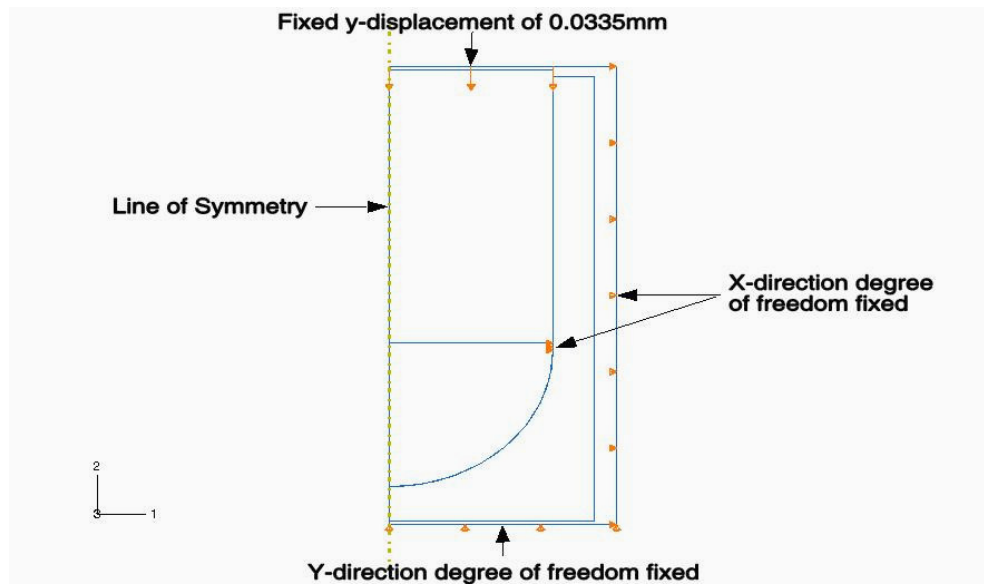


Figure 22. Boundary conditions used for the model of Section 3.2.1.1 are x-direction degrees of freedom are fixed on the outer matrix wall because there exists a symmetry plane and the y-direction degree of freedom on the bottom surface are set to zero. The upper surface has a fixed displacement in y-direction to calculate the stiffness.

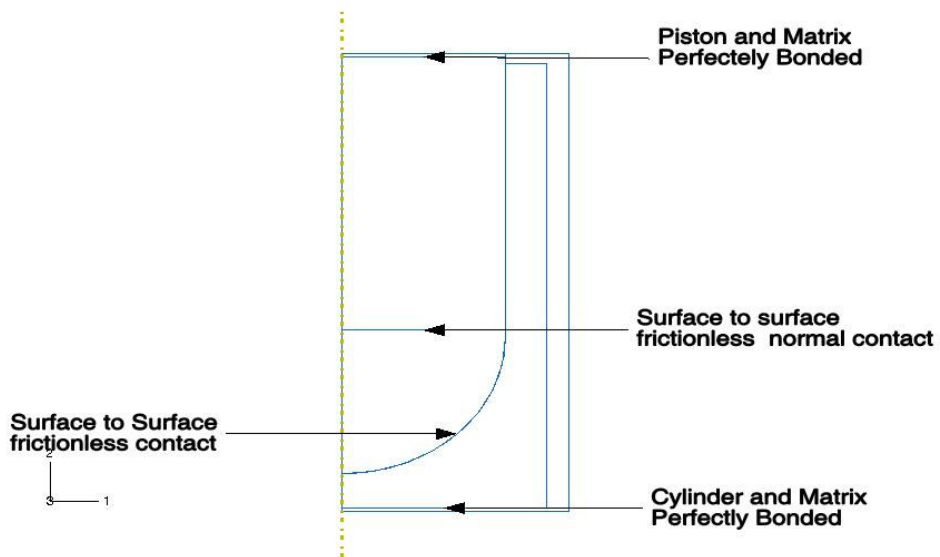


Figure 23. The cylinder and piston head were perfectly bonded using the TIE command in ABAQUS, remaining surfaces have a frictionless surface-to-surface contact.

3.2.1.3. Material Properties and Constitutive Models Used in Analysis

Table 4 shows material properties used in the analysis. Neo-Hookean constitutive model describes the elastomeric matrix material stress-strain response. The neo-hookean model is accurate up to 140% [18]. For an incompressible material only the shear modulus in undeformed position is required. This makes the neo-hookean model favorable because there is no experimental data available.

Elastic modulus for piston and cylinder is 73000 MPa, and the Poisson's ratio is 0.33. This is consistent with Aluminum material properties. The matrix material and incompressible fluid material are incompressible materials with 0.50 Poisson's ratio. The shear modulus for the matrix is 1.41 MPa. The material properties are consistent with polyurethane elastomers [19].

Table 4. Material properties used for the analysis of section 3.2.1 have appropriate modulus and Poisson's numbers.

Part	Modulus (MPa)	Poisson's Ratio
Piston and Cylinder	Young's 73,000	0.33
Matrix	Shear 1.41	0.50
Incompressible Fluid	--	0.50

3.2.1.4. Numerical Results

Figure 24 summarizes the results, and it is evident that as the matrix thickness increases the effective stiffness reduces. The maximum value obtained is 57814.31 MPa at 0.025mm and minimum value is 5920 MPa at 0.075mm. The value at 0.025mm is

favorable and hence this value was used next.

3.2.2. Effective in Plane Stiffness (E_2)

The effective in plane stiffness is calculated in the same way as mentioned in section 3.2.1 and the stiffness at 0.025 mm is taken as E_2 at 0% stroke, that is, 57814.31 MPa.

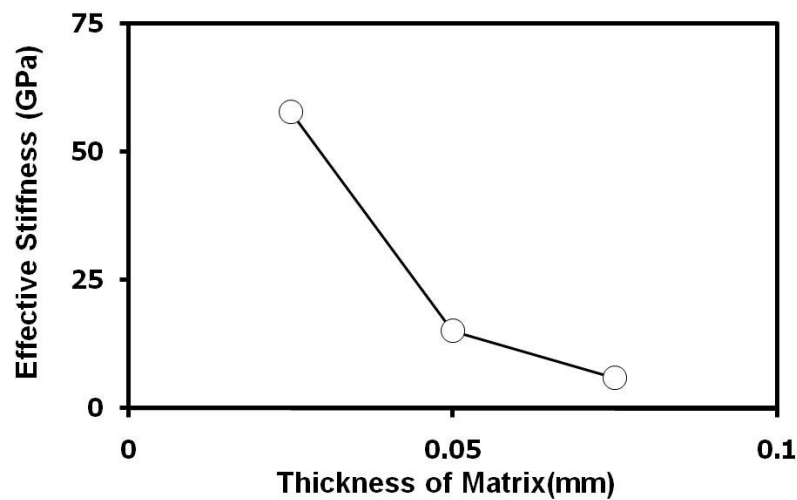


Figure 24. The effective stiffness is directly proportional to the matrix thickness.

The effective in plane stiffness at 50% stroke and 100% stroke is different from the calculation at 0% stroke because the matrix material has to be pre-stretched in this case. For calculating the stiffness at 50% and 100% the incompressible fluid's height is increased. To achieve this, a two-step analysis in ABAQUS is applied. In Step-1, the piston moves to the required stroke by giving a fixed y-displacement and the matrix, which is bonded to the piston and cylinder surface, stretches along with it. In Step -2, a fixed negative y-displacement moves the top surface of the matrix and effective stiffness

is measure as before.

Figure 25 shows the boundary conditions applied for Step 1 and Figure 26 shows the result after Step 1 and the boundary conditions that applied at Step 2. The effective stiffness at 50% is 77,904.75 MPa and at 100% is 94,113.09 MPa.

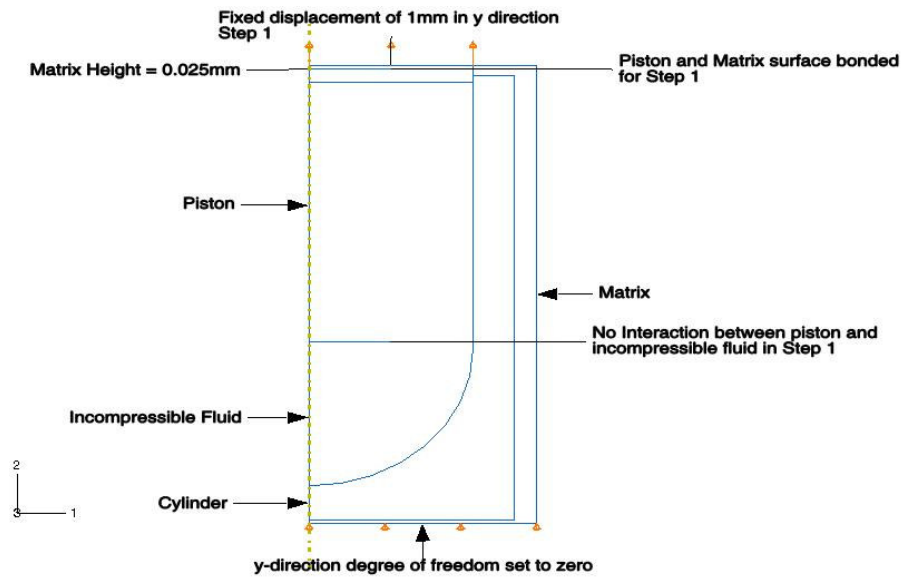


Figure 25. Boundary conditions applied at Step 1 for the analysis of in plane effective stiffness (E_2) at 50% of piston stroke.

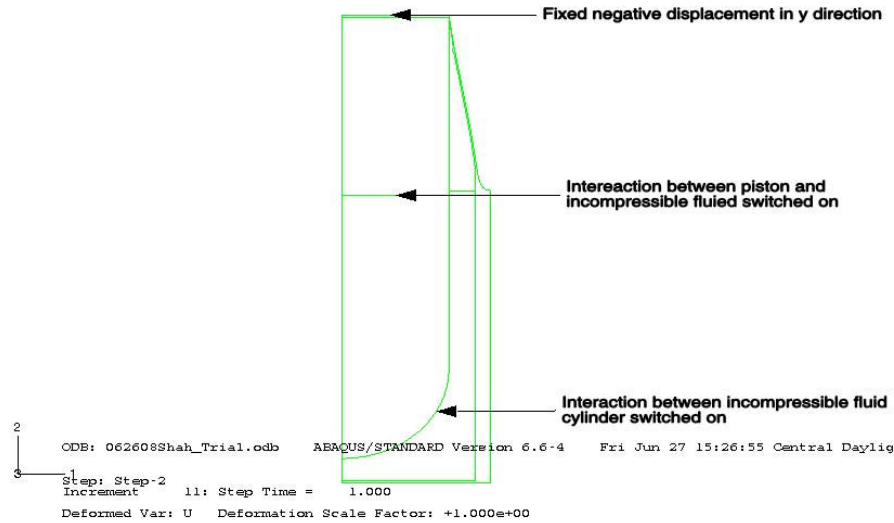


Figure 26. The piston is given a fixed y-displacement to move it to the required stroke,100% in this case, and then a negative y displacement is given on the top matrix surface, the interactions between the piston and incompressible fluid and the incompressible fluid and cylinder are switched on.

3.2.3. Effective Transverse stiffness ($E_1=E_3$) and Poisson's ratio ($\nu_{13}, \nu_{21}=\nu_{23}$)

The effective transverse stiffness is calculated in a similar manner as E_2 , but because using an axisymmetric model would be difficult, a 3-D model is used. Only one-fourth model is used because symmetry planes exist.

3.2.3.1. Boundary Conditions

Figure 27 shows the boundary conditions applied. The bottom surfaces in all the directions have their respective direction displacement set to zero. This is because symmetry planes exist in all these planes. A negative y displacement moves the top surface. The stiffness is calculated in a similar manner as in previous sections. For the transverse Poisson's ratio, ν_{13} , the strain in direction 3 was divided by the strain in direction 1. Strain was calculated by the change in displacement to the original height.

Similarly for the in plane Poisson's ratio, $\nu_{21} = \nu_{23}$, a negative displacement was given in direction 2. The strain in direction 1 was divided by the strain in direction 2.

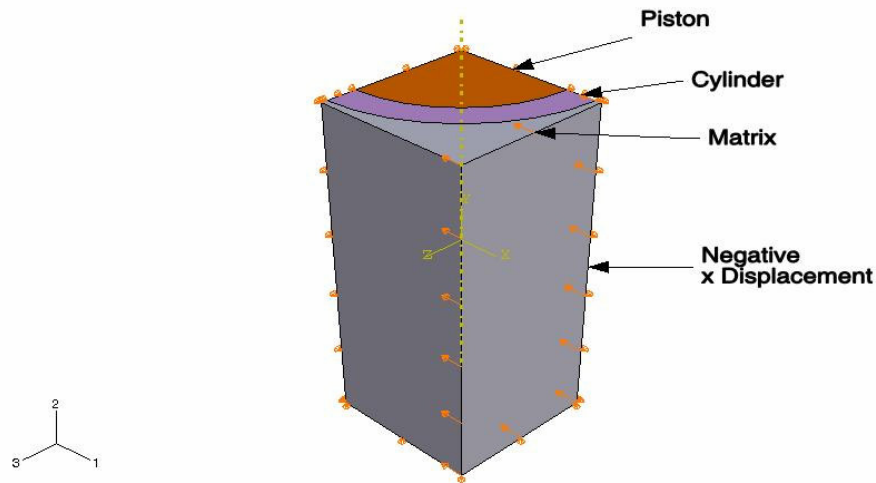


Figure 27. A negative x displacement is given on the right surface and the bottom y surface is fixed in y displacement direction because symmetry exists and similarly bottom planes of 2 and 3 are fixed in y and z directions.

3.2.3.2. Numerical Results

These properties are used in the next section to homogenize a rectangular beam.

Table 5 shows the piston actuator's effective properties.

3.2.4. Effective in Plane Shear Modulus (G_{23})

For calculating the shear modulus, a complete 3-D model was applied because shear force must act on one surface with the other opposite surface fixed. In short, there are no symmetry planes.

3.2.4.1. Boundary Conditions

Figure 28 shows the boundary conditions. The right surface moves in the y-direction and the x-displacement is set to zero. The left surface has both x and y displacement directions set to zero. The sum of all nodal reaction forces on the right surface is divided by the cross sectional area to give the stress. Strain is the right surface x displacements divided by the original height.

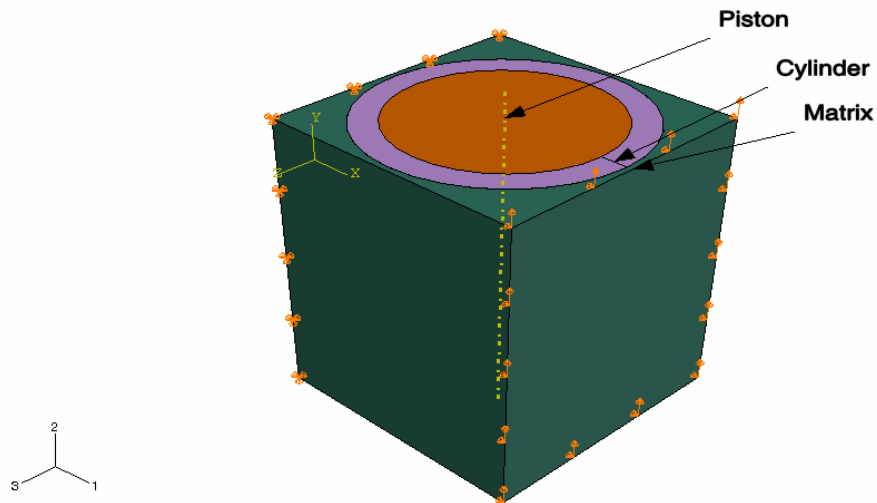


Figure 28. To calculate the shear modulus a complete model is taken as there are no symmetry planes. Boundary conditions to calculate the shear modulus are as shown in the figure.

3.2.4.2. Numerical Results

Table 5 summarizes the piston actuator's material properties. These properties are used in the next section to homogenize a rectangular beam.

Table 5. The Piston actuator's effective properties are transversely isotropic.

Material Property	Value
$E_2(0\% \text{ Stroke})$	57,810.0 MPa
$E_2(50\% \text{ Stroke})$	77,900.0 MPa
$E_2(100\% \text{ stroke})$	94,113.0 MPa
$E_1=E_3$	313.3 MPa
$\nu_{21}=\nu_{23}$	0.437
ν_{13}	0.95
$G_{12}=G_{23}$	124.0 MPa

G_{13} comes from Equation (51) and ν_{12} comes from Equation (49). All the values are within the stability values for a transversely isotropic material as discussed in section 3.2.

Having found the effective properties of a piston actuator, these properties are homogenized in the outer core as shown in Figure 29. Figure 29 also shows the generic beam's cross-section. This cross-section is used in future analysis as 2-D plane strain model. As the cross section remains same throughout the beam's length we can use a 2-D plane strain model. The next section covers the beam's analysis where the work required to twist the beam by 4 degrees is calculated that helps in choosing the actuator's work density. Torsional stiffness of the active beam is compared to a passive beam.

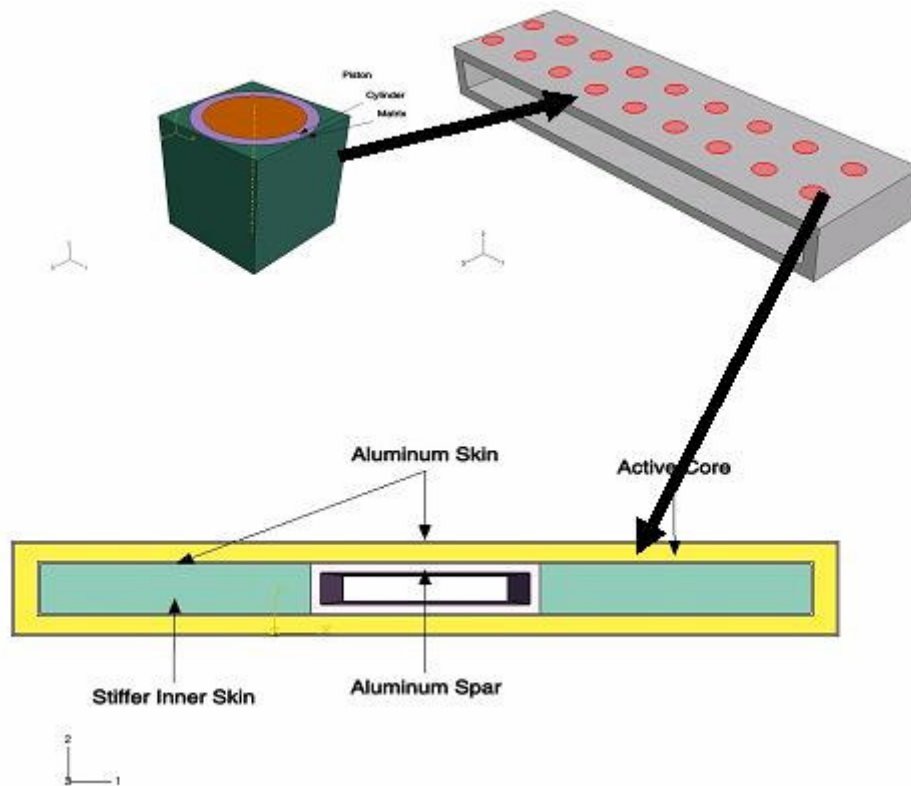


Figure 29. Piston actuator's effective properties are used in the outer active core which is used to twist the beam.

4. ANALYSIS OF GENERIC BEAM

In the previous section, piston actuator's effective properties were calculated. These properties will be used in the outer active core for further analysis. Because we are trying to study how well the piston actuators aid in twist, it is important to find the beam's torsional stiffness. Torsional stiffness is torque per unit deflection. Further sections cover torsional stiffness calculation for a passive beam and an active beam.

Before moving forward, it is important to study as to how the different properties of piston actuators aid in twisting. Figure 30 shows how the piston actuators can twist the beam. To twist the beam a gradual change in the axial deflection along the beam's length is required. The beam's surface at the outer end needs more deflection than the surface near the centre. In addition, one-half the beam has deflections in opposite direction compared to the other half. To achieve this, the piston actuator's effective in-plane stiffness, E_2 , properties are used. Surfaces near the outer end use E_2 at 100% piston stroke and then gradually decreasing towards the center as shown in Figure 30.

Piston actuator's distribution depends on the work required to twist the beam. The work required determines the work density for the piston actuator. To calculate the work required to twist the beam, a polyurethane matrix replaces the active core. This acts as the passive beam, this passive beam acts as a basis for the requirements and comparison. The twist is +/- 4 degrees and the work required to twist the beam by 4 degrees is calculated.

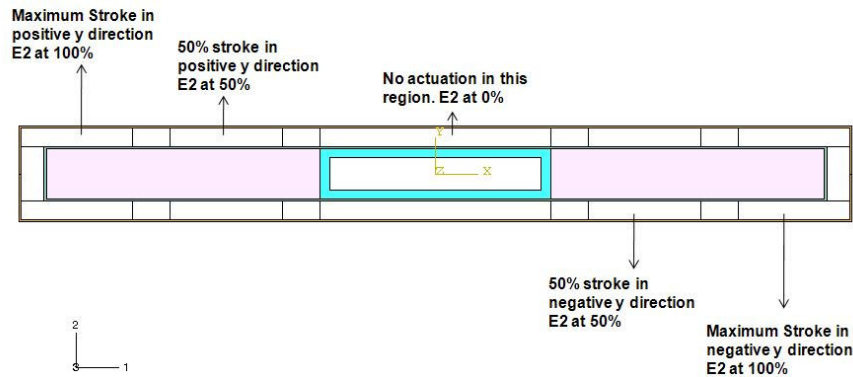


Figure 30. The outer ends of the beam have maximum actuation. As we go towards the center the actuation decreases gradually and thus the result is a couple that helps in twisting the beam. The center part has no actuation and hence only stiffness at 0% is used.

Finite element models are used to analyze the beam. The model used is a 2-D plane strain model as shown in Figure 30. As the beam's cross-section remains same throughout the length, a 2-D plane strain model is a good assumption. As there is anti-symmetry in the load applied, the entire cross-section is modeled. The boundary conditions includes applying two equal and opposite forces on one surface while the other surface has x, y and z displacement directions set to zero. The two equal and opposite forces create a couple, which in turn twists the beam. Near the fixed end, the beam will not twist due to the boundary conditions. Thus, the beam is long enough to keep only 1% of its length in that area. The next section covers this in detail.

4.1. Calculating Beam's Length to Negate End Boundary Conditions

Figure 31 shows the model used for calculating the beam's length. As a start point,

the beam's length is 50mm and incremented in 50mm steps. One end of the beam has all its degrees of freedom set to zero, the other surface has two equal and opposite forces acting on it to create a couple. The load forces act at the center of the outer edges, each node has a 91 N force acting on it. C3D8R, an 8 node hex element available in ABAQUS is used to model the beam. Table 6 shows the material properties used in the analysis. All materials are isotropic except polyurethane, which is a hyperelastic neo-hookean material model.

To negate the end effects 99% of the beam's length should have twist angle per unit length, $\frac{\theta}{L}$, constant. Therefore, $\frac{\theta}{L}$ is calculated along different lengths and for each increment and finally the beam's length was chosen as 3000mm.

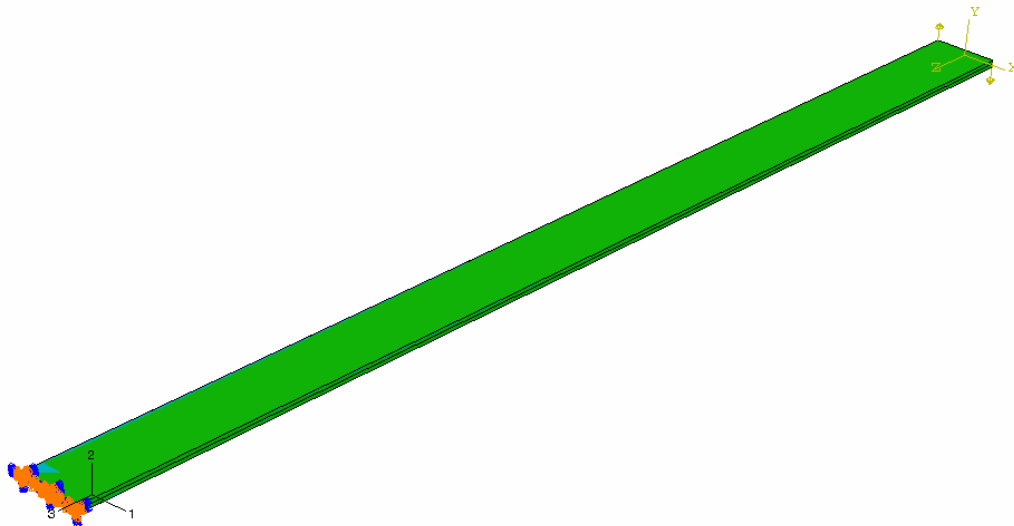


Figure 31. The generic beam has one fixed end and the other end receives two equal and opposite forces that generate a couple.

Table 6. These materials properties were used to analyze the generic beam.

Material	Elastic Modulus (MPa)	Poisson's Ratio
Aluminum 2024 T3	73,000	0.33
Polyurethane	4.24	0.50
Rohacell 110	160	0.33

4.2. Torsional Stiffness and Work Required to Twist Passive Beam

To calculate the work required to twist the beam, the beam twists by 4 degrees and the work required is calculated. This section covers in detail the model, boundary conditions and material properties used for analysis. A 2-D model is used and plane strain assumption is used.

4.2.1. Boundary Conditions

Figure 32 shows the model with boundary condition. The inner surface has x and y displacement degrees of freedom set to zero. Two equal and opposite forces applied at the center of the aluminum skin's outer edges force the twist. Twist angle is calculated after one analysis and then the load is increased until the beam twists by 4 degrees. The ABAQUS TIE keyword bonds all the surfaces.

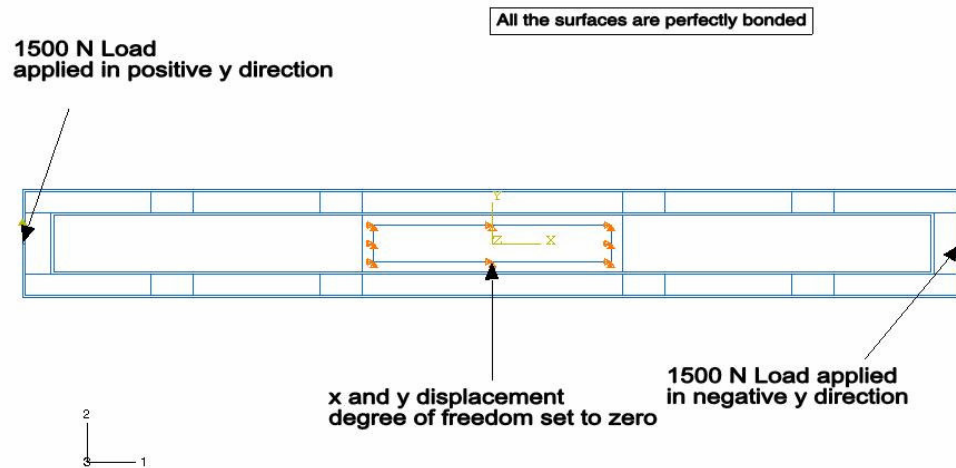


Figure 32. To calculate the work required to twist the passive beam, the x and y displacements are set to zero on the inner surface and 1500 N load is applied at each node at the outer edge to twist the beam by 4 degrees. The ABAQUS TIE keyword bonds all the surfaces.

4.2.2. Element Selection

CPE4R a 2D four node quadrilateral element is used for the outer skins and inner core. The outer core is a hyperelastic neo hookean model. CPE4H a 2D four node quadrilateral element with hybrid formulation is used for analysis.

4.2.3. Material Properties and Constitutive Model

Aluminum material properties are used for the isotropic outer skin. The inner core uses isotropic Rohacell material properties. The outer core uses polyurethane material properties and is a hyperelastic neo hookean material model. Table 6 shows the material properties.

4.2.4. Numerical Results

The load required to twist the beam by 4 degrees is 1500 N. Twist angle, θ , is

calculated using the equation [16]

$$\text{Tan } \theta = \frac{\Delta y}{\Delta x + x} \quad (52)$$

The calculation for the work required appears below.

Load Applied = 1500 N

Twist Moment $T = 1500 \times 180 = 270000\text{N}\cdot\text{mm}$

$\theta = 4 \text{ deg} = 0.0698132 \text{ radians}$

Torsional Stiffness = $T / \theta = 3867.46 \text{ N}\cdot\text{m}/\text{rad}$

Work per unit volume = $0.50 * T * \theta / 3000 = 3.14 \text{ MJ}/\text{m}^3$

The work required to twist the beam indicates what piston-actuator work-density is necessary. Based on the above work required the right material has to be chosen.

Important parameters that are chosen in deciding the material are the material's density and work density. Material's density is an important parameter because if the density is too high it makes the beam very heavy, thus even if high torsional stiffness is achieved the beam would be very heavy. The work density has to be near the work required else, it would make the beam either over-powered or underpowered. The work density for aluminum piston actuators is $7.68 \text{ MJ}/\text{m}^3$. Thus, putting aluminum actuators throughout the core at 50% volume fraction provides the necessary work density. Thus, 50% volume percent is used in future analysis. Also, aluminum is lighter compared to the other materials analyzed and hence aluminum is chosen over other materials.

4.3. Torsional Stiffness of Active Beam

Figure 33 shows the modified beam with 50% of the active core including aluminum piston actuators and the remaining 50% using polyurethane material properties. The

piston actuators are distributed uniformly throughout the beam and the polyurethane matrix acts as a filler material between the piston actuators. The areas marked as PU represent the polyurethane material properties. The boundary conditions used are similar to the boundary conditions in section 0. Because only the torsional stiffness is needed, the load is not changed. Twist angle and torsional stiffness will be calculated.

4.3.1. Material Properties and Constitutive Models Used

The outer core uses the effective piston actuator properties. Table 7 shows the material properties as entered in ABAQUS. All the surfaces in the outer core use only one stiffness value because torsional stiffness at the initial position is required. The piston actuator material is modeled as a transversely isotropic material. The remaining 50% of the outer core modeled as polyurethane is a hyperelastic neo-hookean material model. Aluminum is modeled as isotropic. Table 6 shows aluminum and polyurethane material properties.

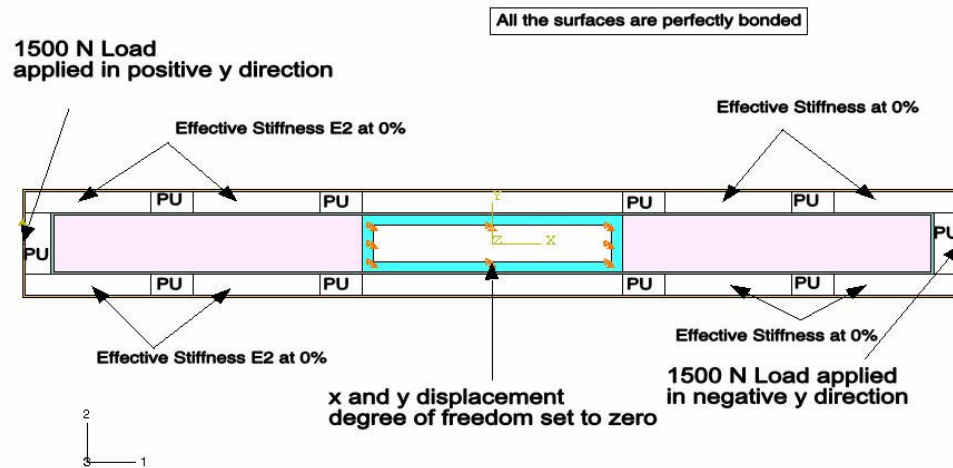


Figure 33. To calculate the torsional stiffness for an active beam at the initial position the active core is homogenized with the effective piston properties. The core is 50% piston actuators and 50% PU. Two equal and opposite forces act on the outer edges.

Table 7. These material properties were used for the piston actuator in the outer core of the active beam.

Material Property	Value
E_2 (0% stroke)	57,814 MPa
$E_1=E_3$	313.2 MPa
ν_{12}	0.0024
ν_{23}	0.437
ν_{13}	0.952
$G_{12}=G_{23}$	124.0 MPa
G_{13}	80.0 MPa

4.3.2. Element Selection

CPE4R a 2D four node quadrilateral element is used for the outer skins and inner core. The outer core and for the only the polyurethane part is modeled as hyperelastic neo hookean model. CPE4H a 2D four node quadrilateral element with hybrid formulation is used for analysis. The anisotropic piston actuator is modeled as CPE4R.

4.3.3. Numerical Results

Figure 34 shows how the applied load and boundary conditions affected the twist. The contour plot shows the displacements. As expected, the displacements are in accordance to how a beam would twist. There are two small bumps at the outer edges at the point where load is applied; this is because polyurethane properties are used at that point. Polyurethane is a soft material and hence the displacement at that point is more. This displacement is small and can be neglected.

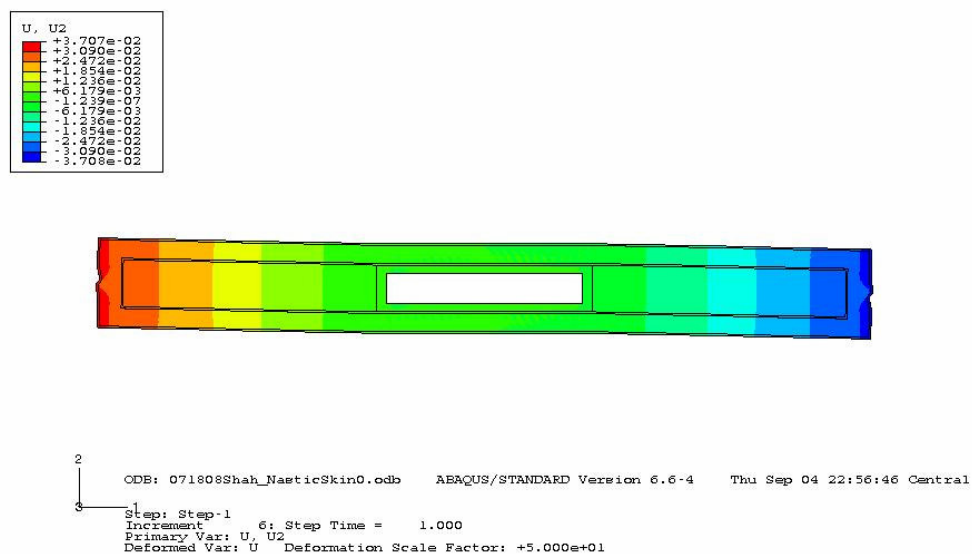


Figure 34. The contour map shows the vertical displacements in the beam.

Torsional stiffness is calculated as below.

Force applied = 1500 N

$T = 1500 \times 180 = 270 \text{ N-m}$

θ calculated using equation (52) = 0.0197 rad

Torsional stiffness = $T/\theta = 13705.58 \text{ N-m/rad}$

4.4. Simulating Active Twist

To calculate the beam's torsional stiffness while twisted and to check the beam's behavior while using the different in-plane effective-stiffness values, E_2 , it is necessary to twist the beam actively. In reality, to twist the beam internal pressure is applied in the piston actuator, but as effective properties are homogenized in the beam, applying internal pressure is not possible. Therefore, to make the beam active, temperature is applied. The thermal coefficient of expansion, α , is constant throughout the beam and temperature variations are applied along the beam. The different stiffness values along the beam's length makes the beam twist due to the deflections caused by temperature changes.

4.4.1. Boundary Conditions

In ABAQUS a predefined field option is used to specify the temperature variation. This allows changing the temperature on the system before applying loads. Figure 35 shows the predefined field applied to the beam. The surfaces on the far right and left are at high temperature and temperature decreases as towards the center. After the predefined field the normal boundary conditions are applied to calculate the torsional stiffness. Figure 36 shows the result and boundary conditions applied after the initial

4.4.2. Element Selection

CPE4R, a 2D plane strain quadrilateral element is used for analysis. All the parts except for polyurethane use the same element. As polyurethane is incompressible, CPE4H a 2D plane strain quadrilateral element with hybrid formulation is used.

4.4.3. Material Properties and Constitutive Models Used

Table 8 shows the effective properties used for the piston actuator in the outer core. Parts of the outer core where polyurethane is used are modeled with a hyperelastic neo-hookean element. Aluminum skins and inner core are modeled as isotropic elements.

4.4.4. Numerical Results

Figure 37 shows the results based on the boundary conditions and material properties used. The torsional stiffness is calculated below.

Force applied = 100 N.

$T = 100 \times 0.180 = 18 \text{ N-m.}$

θ calculated using equation (52) = 1.349148×10^{-3} rad.

Torsional stiffness = $T/\theta = 13341.747 \text{ N-m/rad.}$

Table 8. Effective material properties used for piston actuator that act as a transversely isotropic material.

Property	Value
$E_2(0\% \text{ stroke})$	57,814.0 MPa
ν_{12}	0.0024
$E_2(50\% \text{ stroke})$	77,905.0 MPa
ν_{12}	0.0018
$E_2(100\% \text{ stroke})$	94,113.0 MPa
ν_{12}	0.00145
$E_1=E_3$	313.2 MPa
ν_{13}	0.952
ν_{23}	0.437
$G_{12}=G_{23}$	124.0 MPa
G_{13}	80.0 MPa

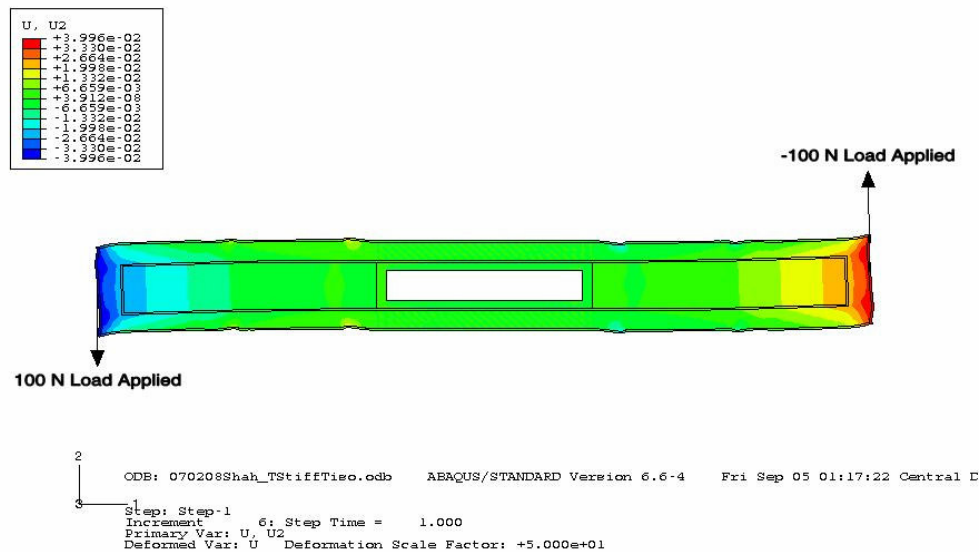


Figure 37. This contour map shows displacements after the forces are applied to the beam.

4.4.5. Result Comparison

Results from previous sections show that the active beam with piston actuators has 3 times the torsional stiffness than the passive beam in the initial state. The active beam's torsional stiffness decreases by 2.6% in the twisted state but it is still approximately 3 times more than the passive beam. Although there is a performance gain in regards to torsional stiffness there is a weight penalty using piston actuators. As aluminum piston actuator's density is high and it being distributed evenly by 50% volume, the active beam's density increases to 1399.42 kg/m^3 compared to passive beam's 1000.01 kg/m^3 .

5. SUMMARY, CONCLUSIONS, AND FUTURE ACTIVITIES

Numerical methods were used to study the piston-actuator behavior and gain knowledge in the geometry, boundary conditions, and material properties that effectively produce piston-actuated nastic materials. From [8] an actuator's performance is measured by blocked stress and free strain, and for the piston actuators in this analysis the blocked stress is almost equal to the material's yield strength.

The piston's size was fixed to a size and the cylinder's outer diameter was designed based on optimum work density. An actuator's work density was chosen based on the amount of work required to twist the passive beam. The maximum work density predicted for steel pistons is 42 MJ/m^3 . The lowest work density predicted in this work was 0.75 MJ/m^3 for nylon pistons. Therefore, we conclude that we can tailor piston-microactuators to meet delivery work density over a broad range. Furthermore, piston-nastic materials can—by keeping the applied pressure less than its maximum—perform with fine control between zero pressure and the design limit pressure.

Having the piston actuators work density database, the work required to twist a passive beam was calculated in order to select the right material for the actuator. The work required shows that aluminum piston actuators distributed 50% by volume best suit the present application. Aluminum was selected on two counts; first aluminum piston actuators work density met the required work. Second, keeping in mind the weight penalty these actuators have and aluminum being lighter than the other materials analyzed, aluminum was selected to the other materials.

Section 4.3 shows that an active beam with nastic materials is stiffer in torsion than a

passive beam. The nastic beam's torsional stiffness is 13.705 MN-m/rad, which is almost three times the passive beam's torsional stiffness. Therefore, we conclude that adding active materials does not compromise torsional stiffness. Indeed, the inner core could be redesigned with lower torsional stiffness and thereby reduce the weight penalty from the nastic outer core.

Section 4.4 shows how the beam twisted actively using temperature variation as a stand-in for pressurization. The torsional stiffness at maximum twist is 13.341 MN-m/rad, which is only 2.6% less than the untwisted torsional stiffness. Therefore, we conclude that the beam can twist without dropping the torsional stiffness significantly.

From the results presented we reach these conclusions:

- Piston-microactuators can deliver work density over a broad range
- Piston-nastic materials perform with fine control between zero pressure and the design limit pressure
- Matrix top layer should be as thin as possible because the effective stiffness decreases rapidly as this layer gets thicker
- Piston-actuator's through-thickness stiffness increases with increasing stroke when an incompressible fluid drives the piston
- Aluminum pistons provide enough work-density to twist the generic beam
- Piston-nastic materials do not compromise torsional stiffness
- Generic beam twists without losing significant torsional stiffness

Future activities should include in looking at piston actuators where the weight penalty can be reduced, that is look at materials with lesser density. The passive beam's

density is 1000.01 kg/m^3 and active beam's density is 1399.42 kg/m^3 . The piston actuators need not be distributed 50% by volume if other materials are analyzed and meet the work requirement. In addition, modeling the actual helicopter blade's aerofoil will help in better understanding and analyzing piston actuators in twisting a blade.

Other applications where piston actuators might be helpful is in morphing a plane's wing. Research is going into developing wings that can change their wing shape. [23] Piston actuators concept might be helpful in helping the shape.

REFERENCES

1. Büter, A, Breitbach E. Adaptive blade twist - calculations and experimental results. *Aerospace Science and Technology* 2000; **4**(5): 309-319.(4).
2. Nastic. (n.d.). Nastic Definition. Dictionary.com Unabridged (v 1.1). <http://dictionary.reference.com/browse/nastic> (accessed March 2008).
3. Thill C, Etches J, Bond I, Potter K, Weaver P. Morphing skins. *The Aeronautical Journal* 2008; **3216**: 117-139.
4. Hawkins GF, Brien M, Zaldivar R, Von BH. Machine augmented composites. *9th International Symposium on Smart Structures and Materials SPIE* 2002; **4698**: 231-236.
5. Shen J, Chopra I. Actuation requirements for a swashplateless helicopter control system with trailing-edge flaps. *43rd AIAA/ASME/ASCE/AHS Structures, Structural Dynamics, and Materials Conference and 10th AIAA/ASME/AHS Adaptive Structures Conference*, 2002:11.
6. Nguyen K; Chopra I. Application of higher harmonic control to hingeless rotor systems. *Vertica* 1990; **14**: 545-556.
7. Wilbur ML, Wilkie WK. Active twist rotor control applications for UAVs. *Proceedings of the 24th US Army Science Conference*, 2006:185-192.
8. Huber JE, Fleck NA, Ashby MF. The selection of mechanical actuators based on performance indices. *Proc R Soc: London* 1997; **A453**: 2185–2205.
9. Belytschko T, Liu KW, Moran B. *Nonlinear Finite Elements for Continua and Structures*. Wiley: New York, 2000.

10. ABAQUS 6.6 Documentation. Hyperelastic material behavior.
ABAQUS/Standard Reference Manual Version 6.6 2006; 4.6.1. (Can be purchased at website <http://www.simulia.com/support/documentation.html>).
11. Wikipedia contributors. Neo-Hookean solid [Internet]. Wikipedia, The Free Encyclopedia; http://en.wikipedia.org/w/index.php?title=Neo-Hookean_solid&oldid=220067213 (accessed July 2008).
12. Senior Aerospace Metal Bellows. PRIME MOVER Metal Bellows Linear Actuator, <http://www.metalbellows.com/Products/primeMover.html> (accessed March 2007).
13. Matweb Material Property Data. Properties of Nylon 6/6,
<http://www.matweb.com> (accessed March 2007).
14. Matweb Material Property Data. Properties of Aluminum 2024 T3,
<http://www.matweb.com> (accessed August 2007).
15. Matweb Material Property Data. Properties of polyetheretherketone,
<http://www.matweb.com> (accessed October 2007).
16. Matweb Material Property Data. Properties of AISI 1006 Steel cold drawn,
<http://www.matweb.com> (accessed November 2007).
17. ABAQUS 6.6 Documentation. Defining Transversely isotropic material.
ABAQUS/Standard Reference Manual Version 6.6 2006; 17.2.1. (Can be purchased at website <http://www.simulia.com/support/documentation.html>).
18. Ogden R. W. Large deformation elasticity-on the correlation of theory and

experiment for incompressible rubberlike solids. *Proceedings of the Royal Society of London. Series A, Mathematical and Physical Sciences* 1972; **326**: 565-584

19. Omotayo FE. Experimentally characterized embedded mckibben muscles as a nastic material for biomedical applications. *Thesis, Texas A & M University*, 2007.
20. Matweb Material Property Data. Properties of Evonik Degussa Rohacell® 110 A Aircraft Grade Polymethacrylimide (PMI) Foam , <http://www.matweb.com> (accessed November 2007).

APPENDIX

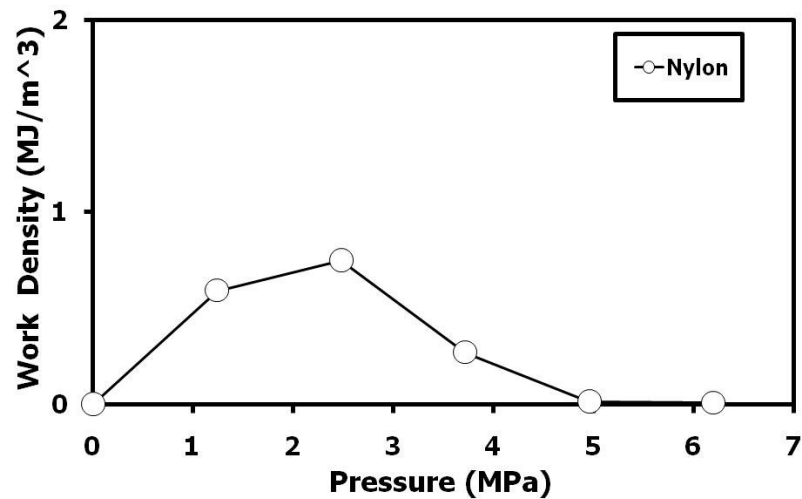


Figure 38. Work density reaches an optimum value as the outer diameter of the cylinder changes to support the operating pressure.

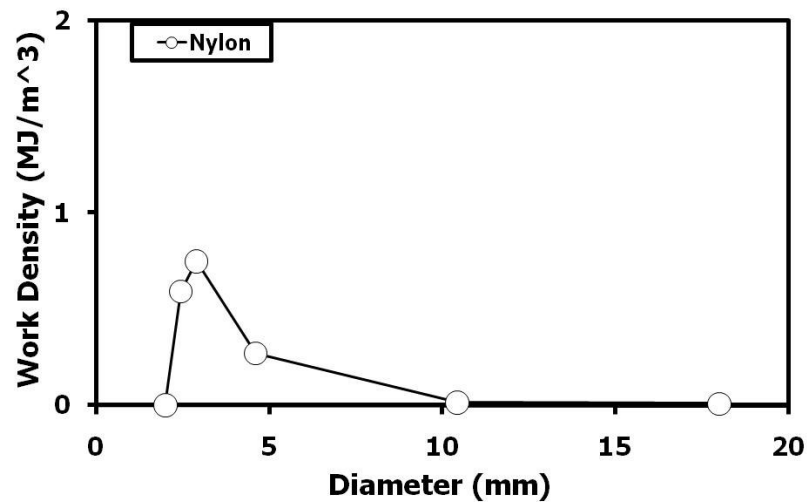


Figure 39. Work density has an optimum value depending on the pressure, which varies from zero to the maximum allowable pressure before the piston starts yielding. In this case the optimum work density is 0.75 MJ/m³.

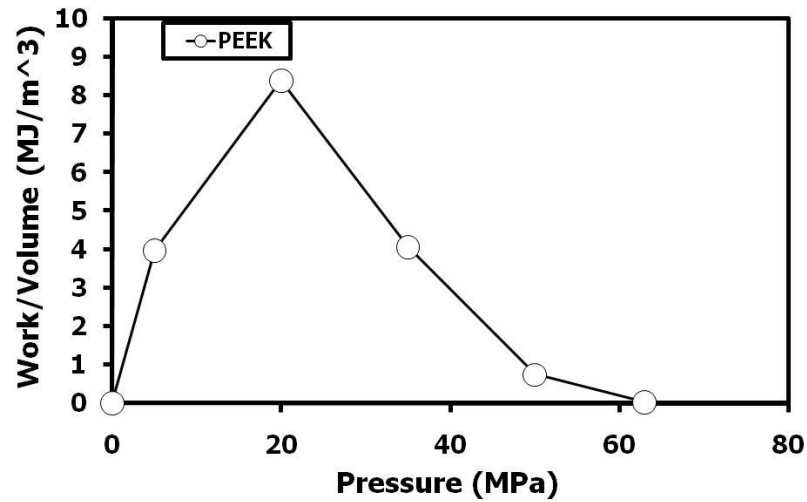


Figure 40. Work density reaches an optimum value as the outer diameter of the cylinder changes to support the operating pressure.

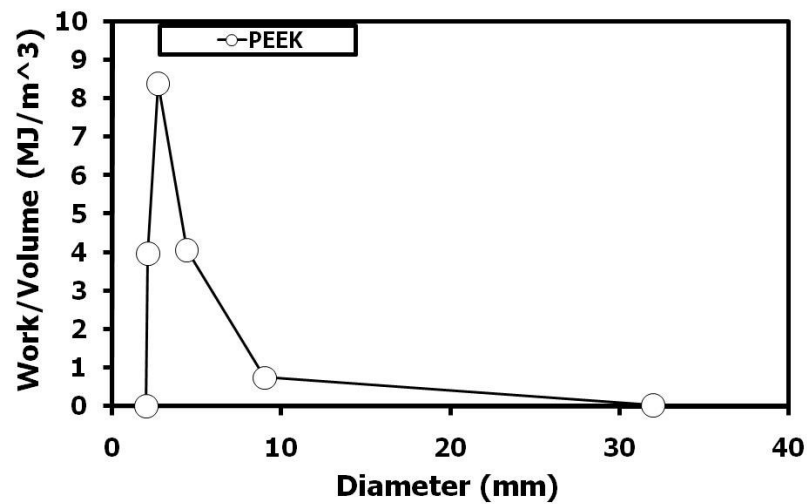


Figure 41. Work density has an optimum value depending on the pressure, which varies from zero to the maximum allowable pressure before the piston starts yielding. In this case the optimum work density is 8.40 MJ/m³.

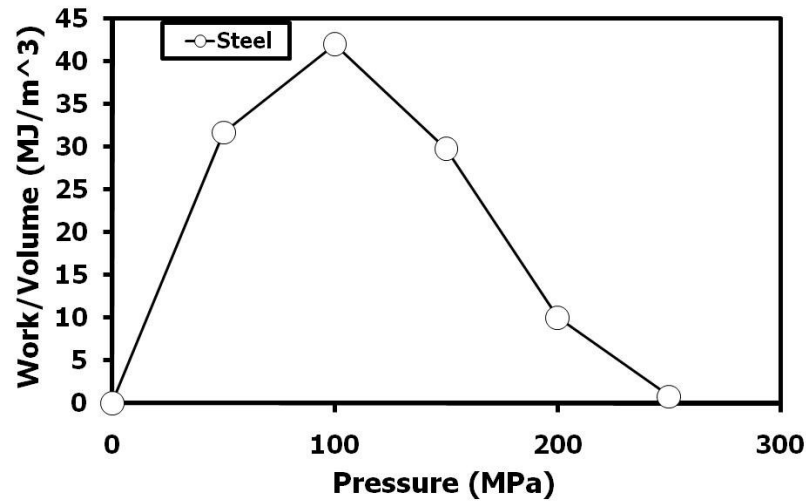


Figure 42. Work density reaches an optimum value as the outer diameter of the cylinder changes to support the operating pressure.

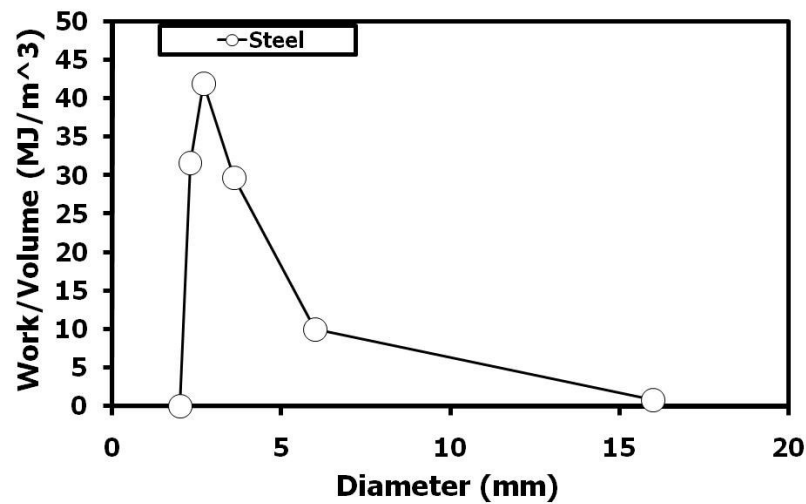


Figure 43. Work density has an optimum value depending on the pressure, which varies from zero to the maximum allowable pressure before the piston starts yielding. In this case the optimum work density is 42 MJ/m^3 .

VITA

Name: Viral Shah

Address: 405, Mayuri Manasa Apts, Behind Visakha Museum.

Visakhapatnam, India 530017.

Email Address: viral320@tamu.edu

Education: B.E., Mechanical Production and Industrial Engineering, Andhra

University, India, 2005

M.S, Mechanical Engineering, Texas A&M University, College

Station, Texas, 2008